RADIO FREQUENCY GAS CHROMATOGRAPHIC DETECTORS

By

HOWARD PERSON WILLIAMS

A DISSERTATION PRESENTED TO THE GRADUATE COUNCIL OF
THE UNIVERSITY OF FLORIDA
IN PARTIAL FULFILLMENT OF THE REQUIREMENTS FOR THE
DEGREE OF DOCTOR OF PHILOSOPHY

UNIVERSITY OF FLORIDA

December, 1966


University of Florida
1853

ACKNOWLEDGMENTS

The author will always be indebted to the people that were influential in the completion of this work. Several were especially helpful and their names should be mentioned.

Deepest appreciation is extended to Dr. James D. Winefordner, Chairman of the author's Supervisory Committee, whose encouragement and understanding have been essential throughout this investigation.

Technical assistance was received from Bill Luchhurst, the machinest.

Many thanks are due to Mr. Tom Glenn for his assistance in the completion of this work.

The author also wishes to express his appreciation to the U.S.A.F. whose financial support made this project possible.

This work could not have been completed without the love and understanding of the author's wife, Joan, and his children, Howard and Michael.

TABLE OF CONTENTS

LIST OF TABLES

LIST OF FIGURES

I. INTRODUCTION

Radio frequency methods of gas detection for gas chromatography date back to 1958 (1). This early detector was only qualitatively described and responded to changes in the dielectric constant of gases flowing through a capacitor. Two matched capacitors were positioned in the same block to eliminate temperature effects. The capacitors were located in tank circuits of two matched oscillators. Only a schematic diagram of the oscillator circuit used was shown. No details concerning the mixer circuit nor the frequency reading device were given. Insufficient data were shown to evaluate and compare this dielectric detector with other gas chromatographic detectors.

In 1961, a vapor detector based on changes in dielectric constant was reported (2). The high frequency circuitry was described in detail, and quantitative results indicated the usefulness of this detector for organic vapors, e.g., acetone, ethyl formate, carbon tetrachloride, and chloroform. Stability, sensitivity, rapid response, and linearity with amount of organic vapor injected were listed as advantages of this detector. This detector was also nearly insensitive to flow rate variation. The detection cell consisted of a capacitor which was part of the resonant circuit of a Clapp oscillator. Two matched oscillators with a mixer circuit and frequency meter comprised the whole detection system. The output of the oscillators was fed into a mixer circuit which relayed the difference frequency to the frequency meter. This detector was

ideal for monitoring gases in flow streams.

Another class of radio frequency detectors uses the properties of a r.f. glow discharge or plasma discharge. Helium or argon are generally used as the carrier gases although other gases could conceivably be used. Helium and argon will support a r.f. glow discharge at atmospheric pressure but reduced pressures are needed for other gases in discharge cell. The dielectric constant of a plasma or a r.f. glow discharge has a dielectric constant less than unity. The relative dielectric constant is given (3) by

$$\epsilon' = 1 - \left(\frac{Wo}{W}\right)^2,$$

where: Wp = angular resonance frequency of the plasma, and

W = angular frequency of the applied voltage.

The resonant frequency of a plasma is affected by many parameters, and any change in this frequency changes the relative dielectric constant. One detector described in this dissertation uses the change in dielectric constant of a plasma as a means of detecting foreign gases in a carrier gas.

There are other means of monitoring changes in the plasma state occurring in a discharge cell. One of these utilizes a probe or probes immersed in the plasma. A probe will have a potential impressed on it depending upon its location in the plasma. This potential is given (3) by

$$\phi(r) = \frac{Xe^2(3r_o^2 - r^2)}{\epsilon_o 8\pi r_o^3}$$

for $r \leq r_o$, where

X = number of electrons and ions

r_o = radius of plasma space charge sphere

r = distance of probe from center of space charge

e = charge on electron or ion, and

ϵ_o = permitivity of free space.

Two probes unsymmetrically situated in the plasma space charge will give rise to a voltage between the two probes (4). It is interesting to note that such an arrangement may be used as a battery. Any change in the carrier gas results in a change in the number of electrons or ions and consequently a change in potential difference between the two electrodes is immediately noted when a foreign gas alters the steady state discharge.

The potential method mentioned above was also used to detect gases. This was very similar in principle to the work reported by Karmen and Bowman (5) who measured the electrical characteristics of a r.f. excited glow discharge in helium to detect organic samples. A d.c. current sufficient to drive a d.c. recorder without amplification was obtained using a highly unsymmetrical cell. A cylinder of wire mesh and a concentrically placed wire were used for the detection cell. The cell was placed in series with a coil, and the d.c. current in this series was monitored. The instrument was quite sensitive to temperature and was 90 percent destructive to organic samples (6). Essentially the same device has been reported by Hampton (7). Winefordner, Williams, and Miller (8) used the same type of circuit as Winefordner, Steinbrecher, and Lear (2); however, the difference frequency corresponded to the changes in a glow discharge occurring in the capacitor cell.

The purpose of this dissertation is to evaluate two types of sensitive r.f. gas chromatographic detectors. One detector has a difference frequency readout, and the other has a d.c. potential difference readout of a probe inserted in the plasma. Both are quite simple in construction, linear in response, and very sensitive.

II. THEORY

A. General Comments

A plasma may be defined (3) as a highly ionized gas composed of positive and/or negative ions, electrons, neutral molecules, and neutral atomic species. In order for a plasma to be maintained at atmospheric pressure, either a high d.c. or a.c. electric field must be present to maintain charge separation and thus the plasma state.

B. Generation of a r.f. Glow Discharge

It is a well-known fact that a glow discharge can be maintained in gaseous helium at atmospheric pressure under the influence of a radio frequency field, such as in the tank circuit of a Clapp oscillator which consists of a series R-C-L circuit (see Figure 1).

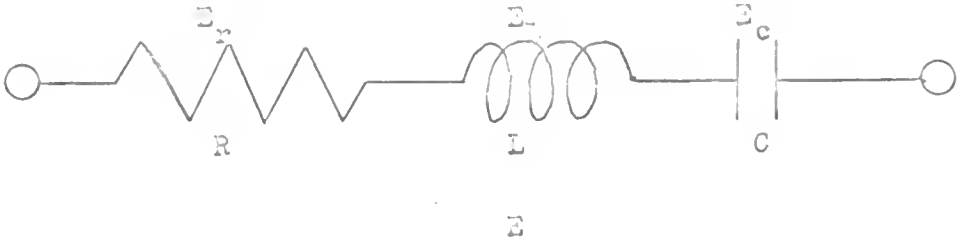

Fig. 1 - Series R-C-L Circuit.

R is the d.c. resistance, L the inductance of the coil, and C the capacitance of the components in Figure 1. This circuit has a resonance frequency when

$$X_c = X_L, \qquad \text{(eqn. 1)}$$

where

$$X_c = \frac{1}{2\pi fC} = \text{reactance of the capacitor} \qquad \text{(eqn. 2)}$$

and

$$X_L = 2\pi fL = \text{reactance of the coil} \qquad \text{(eqn. 3)}$$

The resonant frequency of an R-C-L circuit assuming the d.c. resistance is negligible compared to X_c and X_L is given by

$$f_o = \frac{1}{2\pi\sqrt{LC}} \qquad \text{(eqn. 4)}$$

The total impedance of the resonant circuit is given by

$$Z = \left[R^2 + (X_c - X_L)^2\right]^{\frac{1}{2}}. \qquad \text{(eqn. 5)}$$

The Q, or quality factor, of this circuit at resonance is given by

$$Q = \frac{X_c}{R} = \frac{X_L}{R}, \qquad \text{(eqn. 6)}$$

and in practical circuits Q can have large numerical values, e.g., 100 to 1000. The same amount of current flows through all components of a series circuit, and so at resonance, the voltage drop across C (E_c) and the voltage drop across L (E_L) are given by

$$E_c = IX_c, \qquad \text{(eqn. 7)}$$

and

$$E_L = IX_L. \qquad \text{(eqn. 8)}$$

The voltage, E, across the whole circuit (see Figure 1) is given by

$$E = IZ = IR, \qquad \text{(eqn. 9)}$$

because

$X_c = X_L$ when the circuit is at resonance.

If equations 6, 7, and 9 are combined then

$$E_c = QE, \qquad \text{(eqn. 10)}$$

and so the voltage across the capacitor, C, at resonance can be of the order of hundreds to thousands of volts depending on the applied voltage. Since the spacing between the capacitor plates is small, i.e., less than 1 mm, the voltage gradient can exceed 10,000 volts/cm which is sufficient to produce a r.f. plasma at atmospheric pressure in helium, argon, and other gases.

C. The Resonance Frequency of a Plasma

A plasma has resonance frequencies due to oscillations of ions and electrons. The resonance frequency, f_e, due to electrons (3) (4) is given by

$$f_e = \sqrt{\frac{n_e e^2}{\pi M_e}} = k_e \sqrt{n_e} \qquad \text{(eqn. 11)}$$

where:

n_e = number of electrons per unit volume

e = charge on an electron

M_e = mass of electrons

$k_e = \sqrt{\frac{e^2}{\pi M_e}}$.

A similar frequency expression due to ion motion is given by

$$f_i = \sqrt{\frac{n_i e^2}{\pi M_i}} = k_i \sqrt{n_i} \qquad \text{(eqn. 12)}$$

where:

n_i = number of ions per unit volume

M_i = mass of the ion

$k_i = \sqrt{\frac{e^2}{\pi M_i}}$.

D. The Resonance Frequency of an R-C-L Circuit and its Relationship to Electron Concentration of Plasmas

The resonance frequency of a series R-C-L circuit (3) (4) is changed when a r.f. glow discharge is introduced into the capacitor. The capacitance of the oscillator circuit is given by

$$C = \epsilon' C_o, \qquad \text{(eqn. 13)}$$

where:

ϵ' = real part of the complex dielectric constant

C_o = capacitance with a vacuum between the plates of the capacitor. The dielectric constant for a plasma can be shown to be given by

$$\frac{\epsilon'-1}{\epsilon'+2} = \frac{W_p^2}{W^2p-3W_o^2}, \qquad \text{(eqn. 14)}$$

where:

$W_p = 2\pi f_p$

$W_o = 2\pi f_o$

f_p = resonance frequency of plasma

f_o = resonance frequency of oscillator.

Solving for ϵ' results in

$$\epsilon' = 1-(\frac{W_p}{W_o})^2 = 1- \frac{f_p^2}{f_o^2}. \qquad \text{(eqn. 15)}$$

Now, if the frequency of the plasma, f_p, is taken as the electron resonance frequency, f_e, then

$$f_p = f_e = k_e(n_e)^{\frac{1}{2}}. \qquad \text{(eqn. 16)}$$

Substitution of equation 16 into 15 yields

$$\epsilon' = 1 - \frac{k_e{}^2 n_e}{f_o{}^2}. \qquad \text{(eqn. 17)}$$

Substitution of equation 17 and 4 into equation 13 leads to an imaginary frequency when $W_p{}^2 > W_o{}^2$. For most plasmas at high frequency, this condition is true. Therefore, the simple series circuit described is inadequate to explain the presence of a r.f. discharge in the capacitor of the circuit. However, this problem can be circumvented by using an equivalent circuit to represent the simple series circuit illustrated in Figure 1.

Such a circuit is given in Figure 2. Since the plasma is localized in only one portion of the capacitor, capacitor C can be represented as two capacitors (C_1 and C_2) in parallel, where C_1 represents that portion of the capacitor with no plasma (carrier gas only between the plates), and C_2 represents the portion of the capacitor with plasma.

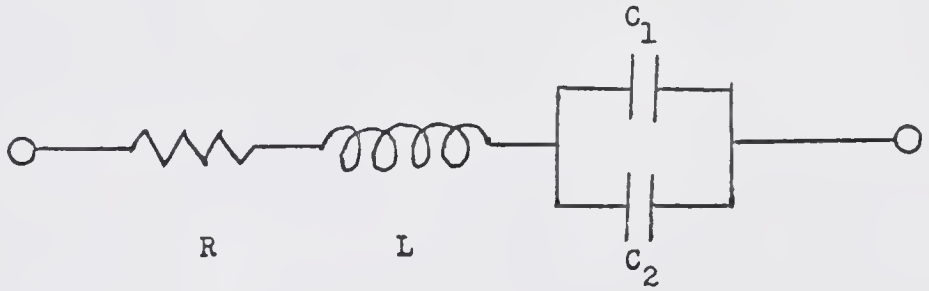

Fig. 2 - Modified Series R-C-L Circuit.

If R (in Figure 2) is very small, then the resonance frequency of the equivalent circuit shown in Figure 2 is given by

$$f_o = \frac{1}{2\pi\sqrt{L(C_1+C_2)}}. \qquad \text{(eqn. 18)}$$

Substituting for C_2 in terms of dielectric constant according to equations 13 and 17 results in

$$f_o = \frac{1}{2\pi\sqrt{L\left[C_1+C_o\left(1-\frac{k_e^2 n_e}{f_o^2}\right)\right]}} \qquad \text{(eqn. 19)}$$

Rearrangement and solving for f_o gives

$$f_o^2 = \frac{1+4\pi^2 LC_o k_e n_e}{4\pi^2(LC_1+LC_o)}. \qquad \text{(eqn. 20)}$$

Differentiation of equation 20 results in

$$2f_o df_o = \frac{4\pi^2 LC_o k_e dn_e}{4\pi^2(LC_1+LC_o)}. \qquad \text{(eqn. 21)}$$

Division of equation 21 by equation 20 gives

$$\frac{2df_o}{f_o} = \frac{4\pi^2 LC_o k_e dn_e}{1+4\pi^2 LC_o k_e n_e}. \qquad \text{(eqn. 22)}$$

Since n_e is of the order of 10^{10} electrons per unit volume, k_e is of the order of 10^4 cps, C_1 and C_o are of the order of 10^{-11} farads, and L is of the order of 10^{-3} henries, then $4\pi^2 L(C_1+C_o)k_e^2 n_e \gg 1$, and so

$$\frac{df_o}{f_o} = \frac{dn_e}{2n_e}. \qquad \text{(eqn. 23)}$$

From equation 23, it can be seen that the change in frequency with respect to a given reference oscillator frequency, i.e., df_o/f_o, is linear with a change in the number of plasma electrons, i.e., $dn_e/2n_e$, with respect to a reference number of electrons. If the relative change in frequency is small, then for a finite change in frequency and electron concentration, the following equation results, namely,

$$\Delta f_o = \left(\frac{f_o}{2n_e}\right)\Delta n_e, \qquad \text{(eqn. 24)}$$

where $f_o/2n_e$ is a constant. This is the equation of a straight line in terms of f_o and n_e having a slope of $f_o/2n_e$.

By taking logarithms of both sides of equation 24, the following equation results

$$\log(\Delta f_o) = \log(\Delta n_e) + \log \frac{f_o}{2n_e}. \qquad \text{(eqn. 25)}$$

This equation indicates a linear plot on log-log coordinates with a slope of unity and an intercept of $\log f_o/2n_e$.

E. <u>The Potential on a Probe Inserted Into a r.f. Plasma</u>

The potential of a spherical plasma which is also related to the electron concentration, n_e, is given by (3).

$$\phi_i(r) = \frac{Xe^2(3r_o^2 - r^2)}{4\pi r_o^3 2\epsilon_o} = \frac{n_e e^2(3r_o^2 - r^2)}{6\epsilon_o} \qquad \text{(eqn. 26)}$$

for $r \leq r_o$ where:

$\phi_i(r)$ = potential on a probe as a function of r

$n_e = \frac{3X}{4\pi r_o^3}$ = number of electrons per cm^3

X = number of electrons in spherical plasma of volume $\frac{4\pi r_o^3}{3}$

e = charge on the electron

r_o = radius of plasma

ϵ_o = dielectric constant of free space

r = distance of a point from the center of the plasma

Thus, if a probe is placed at any point into the plasma, the potential on this probe is given by equation 26. If a second probe is inserted into the plasma, its potential will be described by a similar expression. Therefore, the potential difference between the two probes is given by

$$V_i = \phi_i(r_1) - \phi_i(r_2) = \frac{n_e e^2 (3r_o^2 - r_1^2)}{6\epsilon_o} - \frac{n_e e^2 (3r_o^2 - r_2^2)}{6\epsilon_o}, \quad \text{(eqn. 27)}$$

and so

$$V_i = \frac{n_e e^2 (r_2^2 - r_1^2)}{6\epsilon_o}. \quad \text{(eqn. 28)}$$

By fixing the probes such that r_1 and r_2 are constant and differentiating with respect to n_e, the following equation is obtained

$$dV_i = \frac{e^2 (r_2^2 - r_1^2)}{6\epsilon_o} dn_e. \quad \text{(eqn. 29)}$$

If equation 29 is divided by equation 28, then the relative change in potential difference is given by

$$\frac{dV_i}{V_i} = \frac{dn_e}{n_e}. \quad \text{(eqn. 30)}$$

The interpretation of equation 30 is quite analogous to the interpretation of equation 23. It can be seen that a change in the number of electrons, dn_e, with respect to a reference number, n_e, results in a linear change in the potential difference between the two probes, dV_i, with respect to a reference potential difference, V_i. If the relative change in potential difference, dV_i/V_i, is small, then for a finite change in electron concentration, Δn_e, and in potential difference, ΔV_i, the following equation results

$$\Delta V_i = \left(\frac{V_i}{n_e}\right) \Delta n_e, \qquad \text{(eqn. 31)}$$

where V_i/n_e is a constant for any given r.f. plasma. Equation 31 is the equation of a straight line in terms of ΔV_i and Δn_e with a slope of V_i/n_e. By taking logarithms of both sides of equation 31, equation 32 results.

$$\log(\Delta V_i) = \log(\Delta n_e) + \log(V_i/n_e). \qquad \text{(eqn. 32)}$$

A plot of log (ΔV_i) versus log (Δn_e) should result in a straight line of unity slope and an intercept of log (V_i/n_e)

F. Theoretical Comparison of the Difference Frequency and Potential Difference Methods for Measuring the Change in Electron Concentration of a r.f. Plasma

The two methods of monitoring changes in the number of electrons of a plasma may be compared with respect to relative sensitivity by rearranging equation 24 to give

$$\frac{\Delta f_o}{f_o} \Big/ \frac{\Delta n_e}{n_e} = \frac{1}{2}, \qquad \text{(eqn. 33)}$$

and by rearranging equation 31 to give

$$\frac{\Delta V_i}{V_i} \Big/ \frac{\Delta n_e}{n_e} = 1. \qquad \text{(eqn. 34)}$$

From equations 33 and 34, it can be seen that the change in frequency with respect to a reference frequency is half as great as the change in potential difference with respect to a reference potential difference for the same relative change in electrons. Therefore, the change in potential difference method should be twice as sensitive as the change in frequency method.

G. Application of Expressions to Gas Chromatographic Systems

The carrier gas used in most of the studies was helium (He) although several other gases, including argon, could be used. The r.f. glow discharge in helium results from the excitation of He atoms to an excited state (He^*) via the r.f. energy. Since even the highest purity helium contains ionizable impurities (I), there is a background electron concentration (n_e) due entirely to the carrier gas, which can be represented as

$$He^* + I \rightarrow He + I^+ + e^-(n_e). \qquad \text{(eqn. 35)}$$

When a sample is put into the r.f. discharge, the sample may or may not fragment into smaller radicals due to the high energy of the He^* particles, and the resulting particles can either ionize due to collisions with the metastable heliums which will cause an increase of n_e to $n_e + \Delta n_e$ or capture electrons resulting in a decrease of n_e to $n_e - \Delta n_e$. If more than one fragment results part of the resulting particles can

ionize and part can capture electrons, and so the change in n_e cannot be predicted unless the specific case is known. If the sample (S) is not fragmented but is ionized, the process can be represented as

$$He^* + S \rightarrow He + S^+ + e^-(+\Delta n_e). \qquad \text{(eqn. 36)}$$

If the sample (S) is not fragmented but captures electrons, the process can be represented as

$$S + e^- \rightarrow S^- \quad (-\Delta n_e) \qquad \text{(eqn. 37)}$$

Therefore, a change in electron concentration, Δn_e, results due to the sample (or its fragmented products) ionizing or capturing electrons. The change should be a linear function of the amount of sample, S_a, introduced into the gas chromatographic column if the above processes are correctly depicted, i.e.,

$$\Delta n_e = K_c S_a, \qquad \text{(eqn. 38)}$$

where K_c is a function of the plasma, the sample molecule, and the column size, temperature, and characteristics. Therefore, as long as all experimental conditions are maintained constant and change in n_e, V_i and f_o are small, then

$$\Delta f_o = \frac{f_o K_c S_a}{2n_e}, \qquad \text{(eqn. 39)}$$

and

$$\Delta V_i = \frac{V_i K_c S_a}{n_e}, \qquad \text{(eqn. 40)}$$

which indicates a linear relationship between the signal and amount of sample being measured.

III. EXPERIMENTAL

A. Sampling Technique for Gases

The sampling device chosen was an exponential dilution flask first described by Lovelock (9). In principle, it consisted of a chamber of a fixed volume with an inlet for the carrier gas, an injection port for sample introduction, a mixing device to instantaneously mix the sample plus carrier homogeneously, and an exit port. The expression for concentration, C, at any time, t, should be given by:

$$C = C_o \exp(-\frac{Ut}{V}) ,$$

where V = volume of flask (cm^3)

U = flow rate (cm^3/sec)

t = time (sec)

C_o = concentration at t = 0

C = concentration at any time, t

The plot of log C versus time gives a straight line with a slope of $-\frac{U}{2.303V}$ and an intercept of log C_o.

The construction of the dilution flask was non-critical. A schematic drawing of the flask is given in Figure 3 and the construction procedure is as follows. A phenolic cylinder (3) was turned on a lathe to the following dimensions: 3 in.(o.d.) x 1/4 in.thick x 2 3/4 in.high. The end pieces (4) were cut from 1/4 in.thick sheet LUCITE (R). An 11/64 in.x 1/8 in.deep hole was drilled in the center of each end piece to act as a bearing for the paddle assembly.

Fig. 3 - Exponential Dilution Flask Used for Sampling.

1. Magnetic Stirring Bar
2. Teflon Vanes
3. Phenolic Cylinder
4. Lucite End Pieces
5. Injection Port
6. Photo Spool With Teflon Bearings
7. Copper Tubing

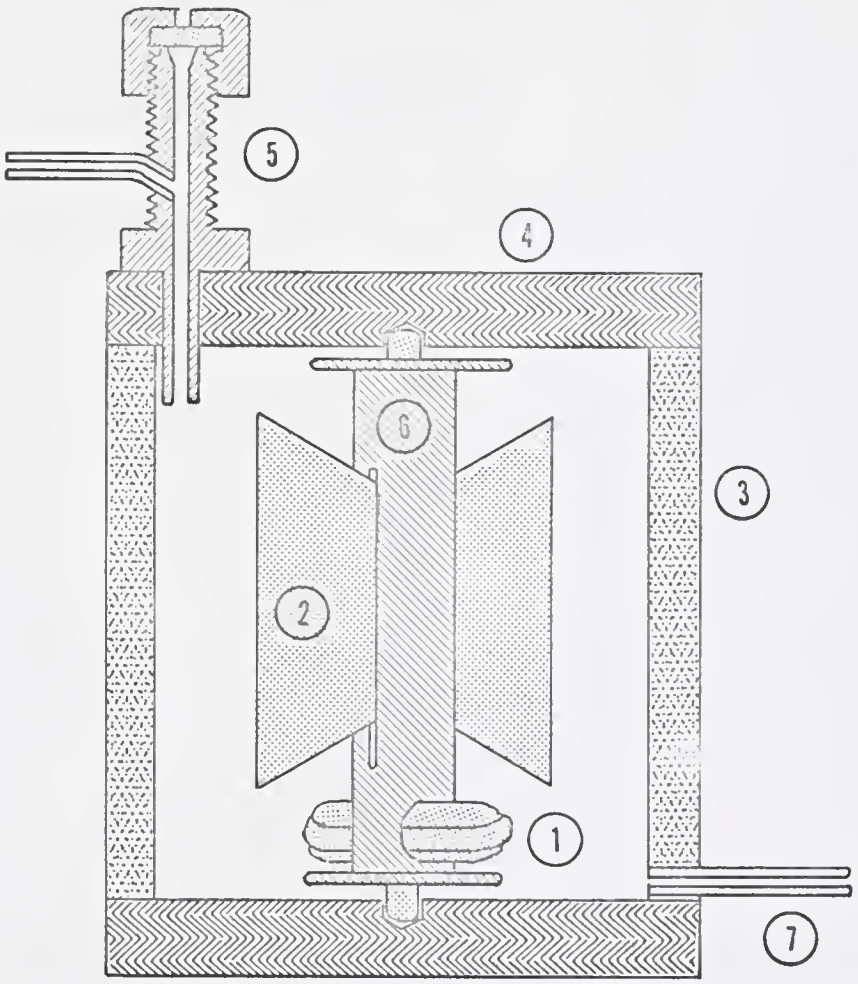
5
4
6
3
2
1
7

The paddle assembly was constructed by cutting trapezoidal shaped vanes, 1 1/2 in.x 1 in.x 1 in.high, from 1/32 in thick TEFLON ® sheet (2). These were inserted into a size 120 plastic roll film spool (6) (Supreme Photo Supply Co., Inc., 1841 Broadway, New York,23, N. Y.). A TEFLON ® covered magnetic stirring bar (1) was inserted into a 5/16 in. hole which had previously been drilled in the film spool perpendicular to the slots and about 1/4 in.from the end. The vanes and stirring bar were then cemented in place. A 1/4 in.TEFLON ® rod was turned to 5/32 in.diameter x 1/4 in.and inserted in the ends of the spool to act as the shaft assembly.

The injection port was fabricated from a brass bulkhead adapter SWAGELOK ® (Crawford Fitting Co., 884 East 140th Street, Cleveland, Ohio, part no. 200-A1-2) (5). A 1/8 in.hole was drilled in the side of the injection port, and a piece of 1/8 in.(o.d.) copper tubing (7) was soldered in place. A small round file was used to smooth rough edges inside the injection port, and an injection gasket (Wilkens Instrument & Research, Inc., Box 313, Walnut Creek, California) was held in place as shown in Figure 3. This injection port assembly was then fitted into a 1/8 in.hole which was drilled in an end piece 3/8 in.from the edge and cemented in place. Next, a 1/8 in.exit hole was drilled in the side of the phenolic cylinder 3/16 in.from the base (see Figure 3), and a piece of 1/8 in.copper tubing was cemented in place. Finally, the end pieces were cemented to the phenolic cylinder containing the paddle assembly. There was sufficient room between the vanes and the cylinder wall to prevent any obstruction to a syringe needle. A magnetic stirring

motor completed the assembly. The volume of this particular flask was 219 cc.

All samples were introduced into the dilution flask using Hamilton gas-tight syringes. With the exception of air, plastic bags filled with the particular gas under investigation were used in conjunction with the syringes to avoid contamination of the gas by air. Sandwich size "Baggies" were flushed out several times with the sample gas then the top was twisted tightly to seal the gas in. Next, a short piece of masking tape was pressed around the twisted end to seal permanently the bag filled with gas, and within a matter of seconds, the needle of a syringe was inserted through the plastic bag such that the needle extended into the inner space of the bag. The syringe was flushed several times by filling and subsequently emptying the syringe with the needle inserted in the bag. A positive pressure was maintained on the gas-filled bag to prevent diffusion of air into it through the opening caused by the needle. Next, the bag of gas with the syringe needle still inserted was placed against the injection port of the dilution flask such that the syringe was pointed at the injection port through the bag. The injection was then accomplished by pushing the needle through the other wall of the plastic bag and into the injection port. The gas sample was thus injected with a minimal amount of contamination by air. This method gave reproducible results and was much more reliable than other sampling methods attempted. For injection of samples near the lower limit of detection only one bag per injection was used. However, at other ranges, two or three injections were made

using one gas-filled bag by patching the holes with masking tape. Hamilton syringes with removable needles were found to leak at the needle syringe junction. To prevent this, thin TEFLON® tape was wrapped about the male syringe fitting between needle and syringe. When the needle was pressed on to the syringe with a twisting motion, the TEFLON® flowed and gave a gas-tight seal.

A sampling difficulty encountered with the syringes was due to the soft injection port septums clogging the needles either partially or completely. This problem was eliminated by changing needles often.

B. The Frequency Detector

A block diagram of the experimental setup is given in Figure 4. The resonant frequency of the sample and reference oscillators was 72 Mc. Clapp oscillators were similar to the ones previously described by Winefordner, Steinbrecher, and Lear (1). The outputs of each oscillator were fed into a diode mixer circuit. Due to the tendency for the oscillators to capacitatively couple at these high frequencies, an attentuation network consisting of C_7 and R_4 in Figure 5 was used to lower the oscillator output voltage to 0.2 volts as measured with a Hewlett Packard Model 410-B Vacuum Tube Voltmeter. This combined with good shielding resulted in a minimal amount of "lock in." Cathode followers were found to be useless at these frequencies.

The output of the mixer was fed into the frequency meter and then into a recorder. The oscillator circuit used for both detectors is shown in Figure 5. The circuit of the mixer circuit is given in Figure 6, and the circuit of the frequency meter circuit is described in Figure 7.

Fig. 4 - Block Diagram of Frequency Detector.

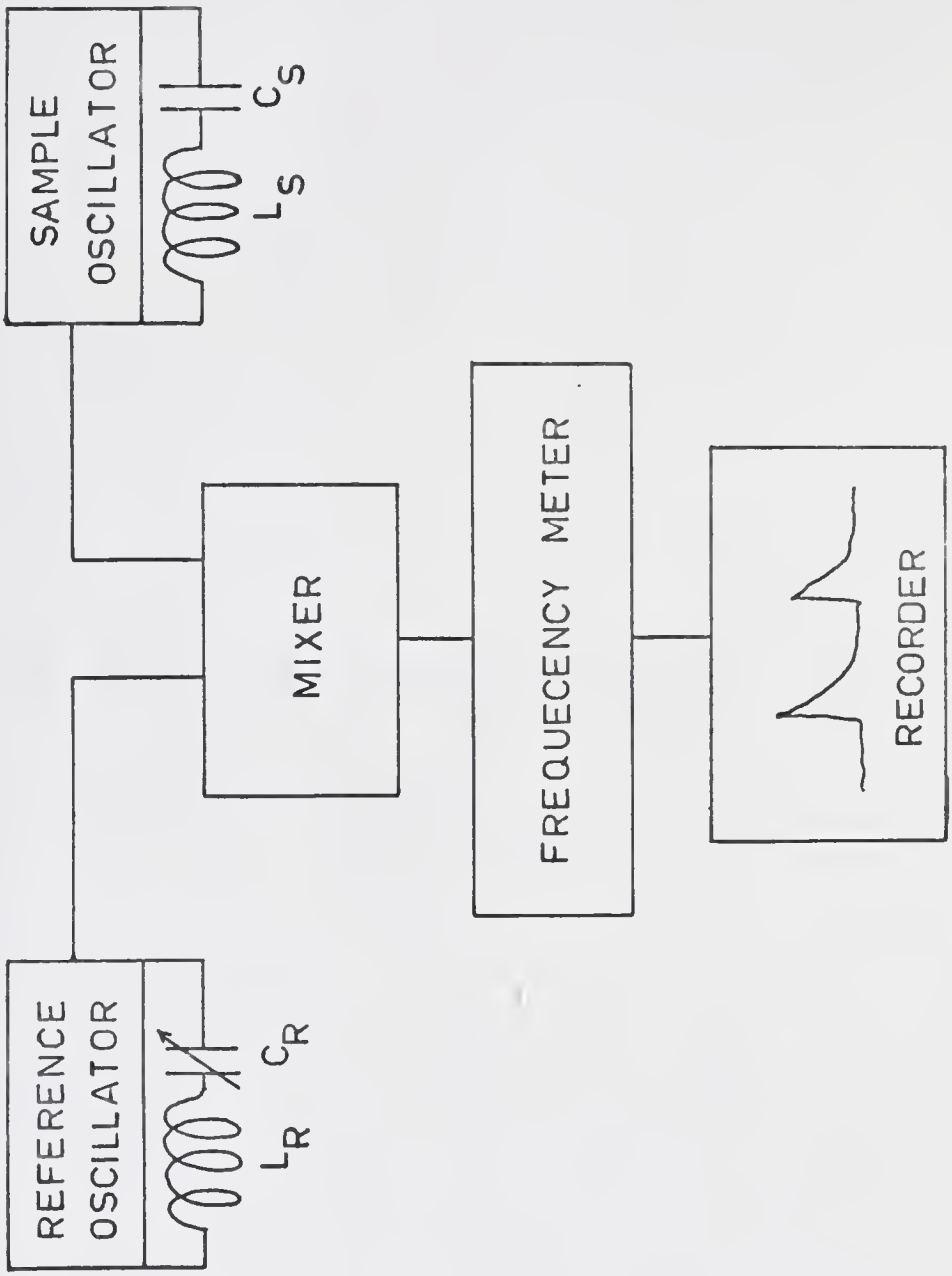
SAMPLE OSCILLATOR
L_S
C_S
REFERENCE OSCILLATOR
L_R
C_R
MIXER
FREQUECENCY METER
RECORDER

Fig. 5 - Schematic Diagram of Oscillator for Frequency Detector.

R_1 - 12k

R_2 - 33.2k

R_3 - 64k

R_4 - 47k

C_1 - 1.8-13 pf

C_2, C_3 - 50 pf

C_4 - detector cell

C_5, C_6 - 2700 pf

C_7 - 1.8-13 pf

L_1 - 7-8 turns on 4 x 3/4 in diameter form

L_1 - 7-8 turns of No. 10 silvered copper wire on a 4 in x 3/4 in diameter syrene form

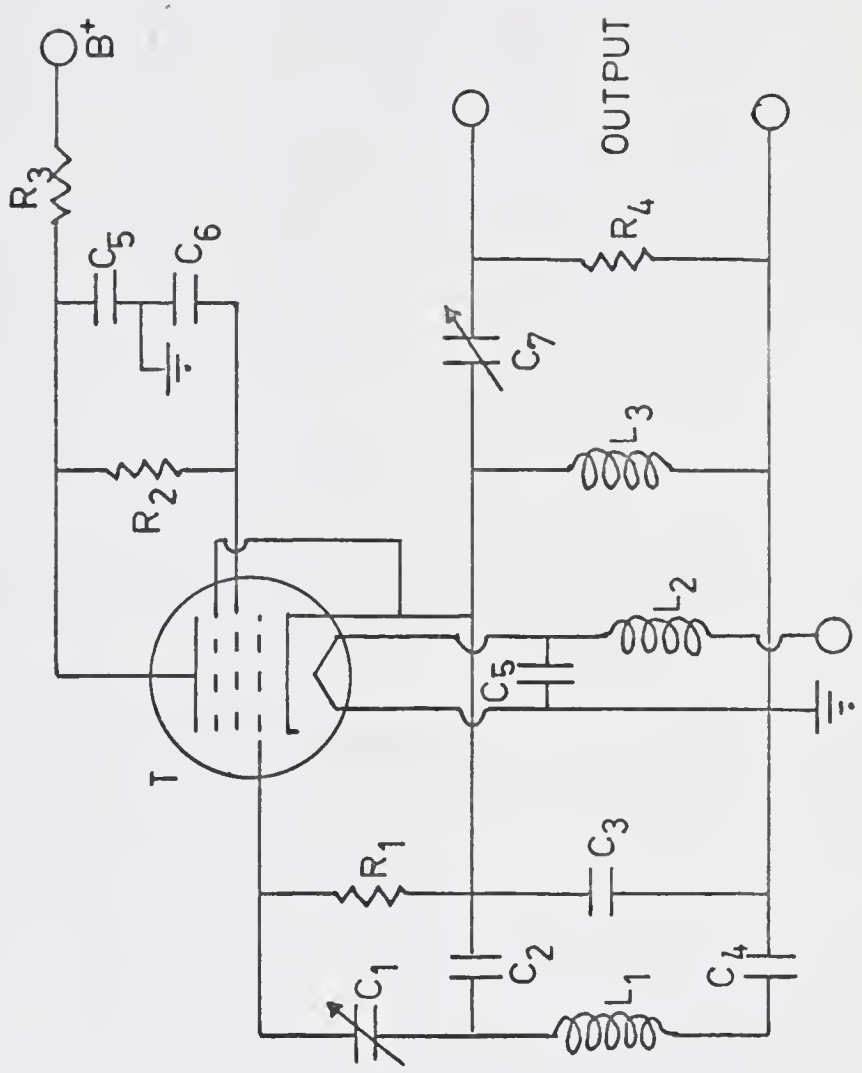
B+
R3
C5
C6
R2
T
R1
C1
C3
C2
L1
C4
C7
L3
R4
OUTPUT
L2
C5

Fig. 6 - Schematic Diagram of Mixer Circuit for Frequency Detector.

C_1, C_2 - 100 pf

C_3, C_4 - 220 pf

C_5, C_8 - 0.01 mfd

C_6 - 0.001 mfd

C_7, C_{14} - 1.5-3 pf

C_9 - 10 pf

C_{10} - 0.001 mfd

C_{11}, C_{12} - 100 pf

C_{13} - 16 mfd elect.

R_1, R_2 - 1 meg

R_3, R_4 - 180

R_5, R_7 - 22k

R_6 - 12k

R_8 - 7.5k

R_9 - 13k

R_{10}, R_{11} - 100k

L_1 = 10uH r.f. choke

L_2 = Two sections in parallel 7 turns each, 32/in. 1/2 in. form • 0.6 in. between sections

L_3 = 5 turns, 32/in. between sections of L_1

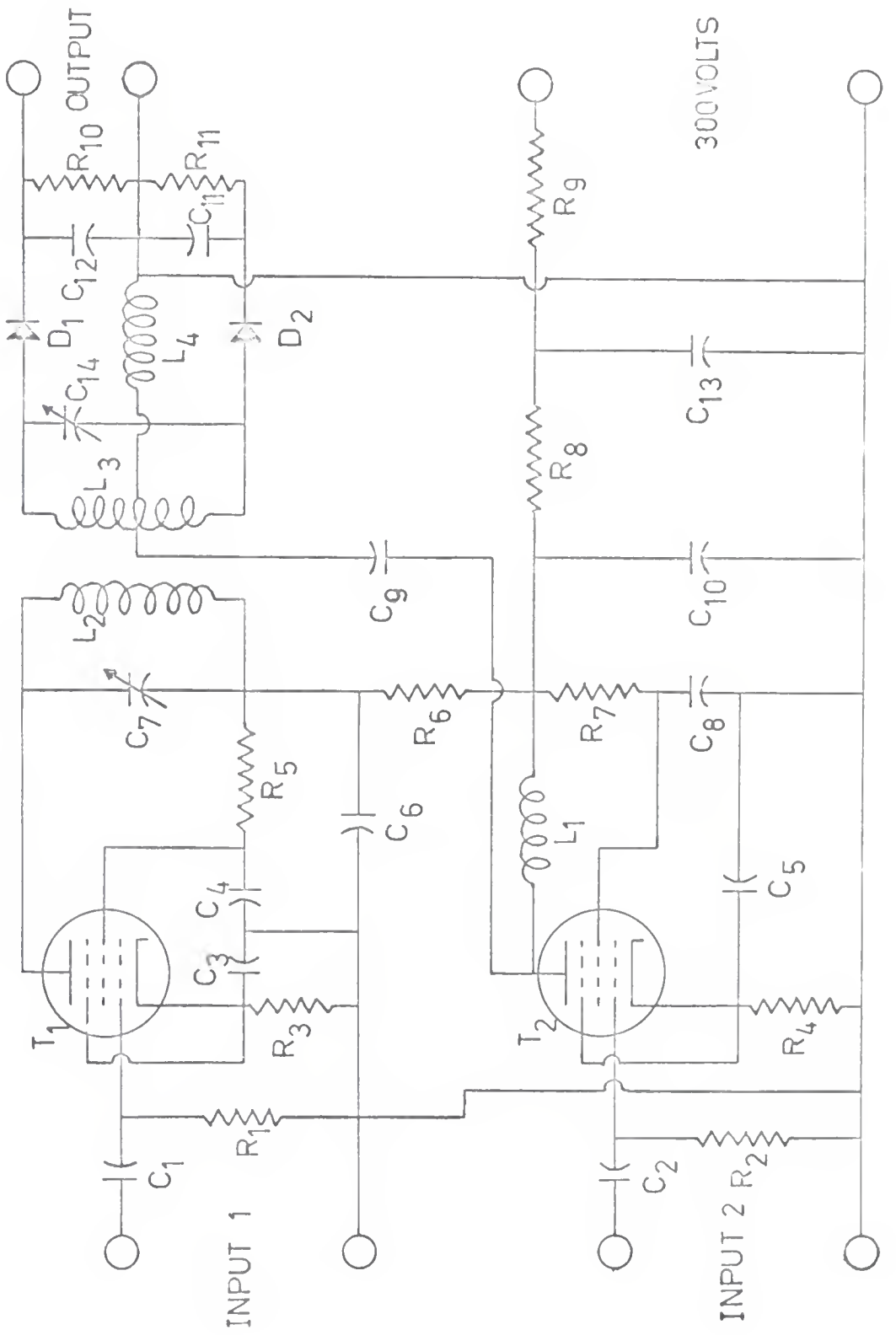
OUTPUT
300 VOLTS
INPUT 1
INPUT 2
R10
R11
C12
C11
D1
D2
L4
C14
L3
L2
C7
R5
C6
C9
R6
R9
R8
C13
C10
R7
C8
L1
C5
C4
C3
T1
T2
R3
R4
R1
R2
C1
C2

Fig. 7 - Schematic Diagram of Frequency Meter for Frequency Detector.

R_1 - 670k

R_2 - 180

R_3, R_7 - 22k

R_4, R_8 - 10k (10 watt)

R_5, R_9 - 470k

R_6 - 220

R_{10}, R_{11} - 4.7k

R_{12} - 15k

R_{13} - 37k

R_{14} - 5.6k

R_{15}, R_{16} - 5k

R_{17} - 15k (10 watt)

R_{18} - 1k (10 watt)

R_{19}, R_{20} - 1.3k

R_{21} - 2

C_1, C_4, C_7 - 0.25 mfd

C_2, C_3, C_5, C_6, C_8, C_9, C_{10} - 20 mfd elect.

1 - 22

2 - 50

3 - 0.0001

4 - 0.00025

5 - 0.0005

6 - 0.001

7 - 0.002

8 - 0.005

9 - 0.01

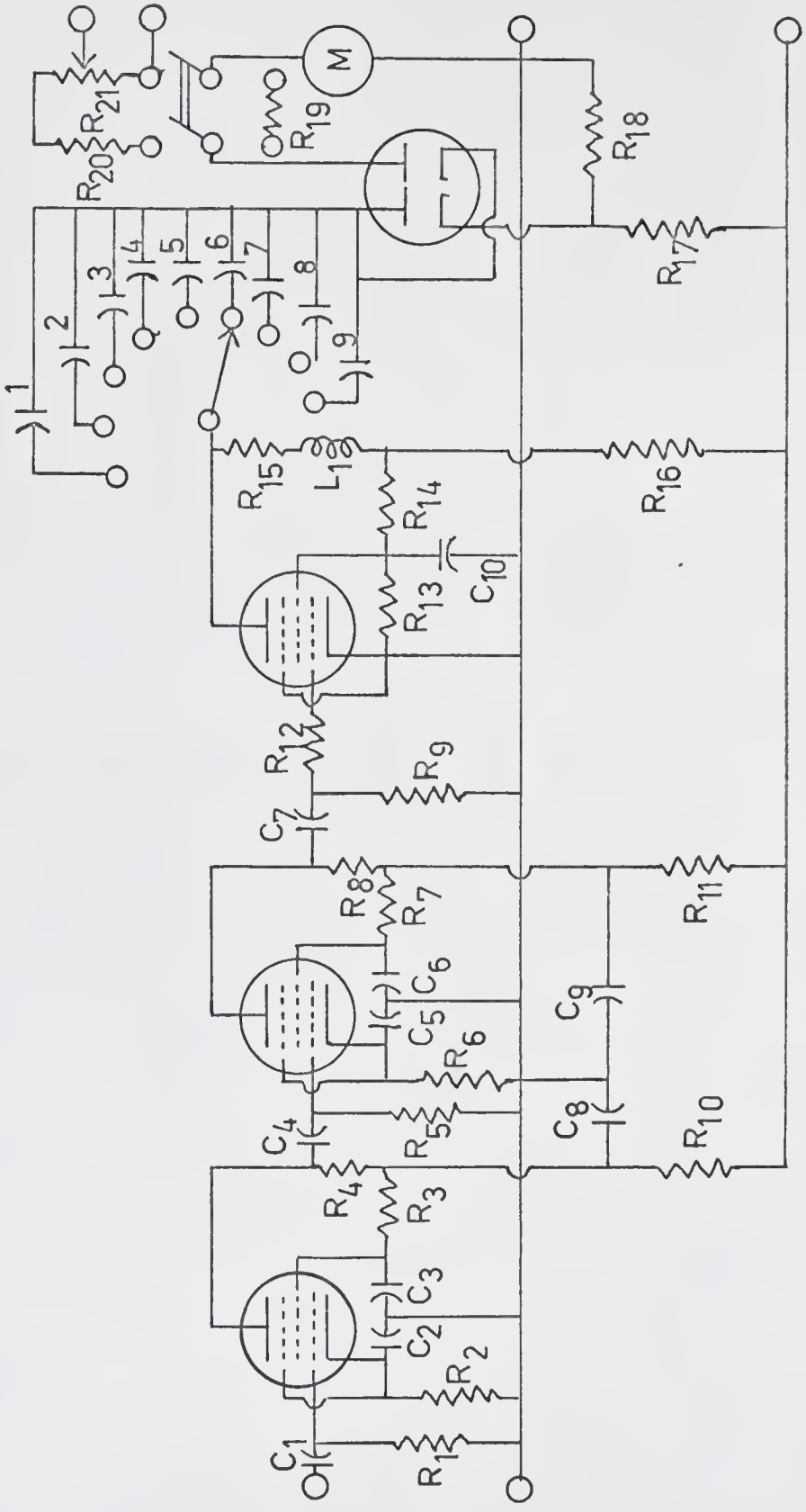
M
R21
R20
R19
R18
R17
R16
R15
L18
R14
R13
C10
R12
R9
C7
R8
R7
C6
C5
R6
C9
R11
C4
R5
C8
R10
R4
R3
C3
C2
R2
C1
R1
1
2
3
4
5
6
7
8
9

The values of all components are listed in the captions for each diagram. The Clapp oscillators were built on aluminum chassis (3 x 6 x 4 inches). The coil L_1 in the tank circuit was rigidly mounted on a porcelain plate on the top of the chassis and was shielded by means of an aluminum box (3 x 4 x 3 inches). The oscillator tubes were enclosed in tube shields. The B^+ and filament connections for the oscillators were connected to 500-μμf button-type feed-through condensers and r.f. chokes (Ohmite Z-50) and then to regulated power supplies. The feed-through condensers and the chokes are not shown in Figure 5. A regulated power supply (Model 407D, John Fluke Mfg. Co., Inc., Seattle, Washington) was used to supply the power to the filaments and B^+ of the oscillators. A regulated power supply (Model PS-3, Heath Co., Benton Harbor, Michigan) was used for the mixer and frequency meter. It was of great importance that the components of the tank circuits be mounted and wired as rigidly as possible. Square bus bar wire was used for all connections in the tank circuit. The coils were wound from silver-coated copper wire (No. 10) and were mounted rigidly on polystyrene rods (3/4 in.o.d.). Connections to the coils were made through the base of the porcelain plate. The leads of all components were kept short and positioned as far from the chassis as possible to avoid loss of energy from the circuit due to capacitative effects.

The cell capacitor, drawn to scale, is shown in Figure 8. It consisted of a micrometer ⑥ (No. 263, L. S. Starrett Co.,) mounted in a brass cylinder 1/2 in.i.d. x 3/4 in.o.d. x 3 5/8 in.long. The cylinder was threaded to fit into a 3 in.o.d. by 1/2 in.thick brass mounting

Fig. 8 - Detector Cell for Frequency Detector.

1. Carrier plus sample gas inlet
2. Carrier gas inlet
3. Mounting flange
4. Coil side of cell
5. Housing for cell
6. Micrometer
7. TEFLON® bushing

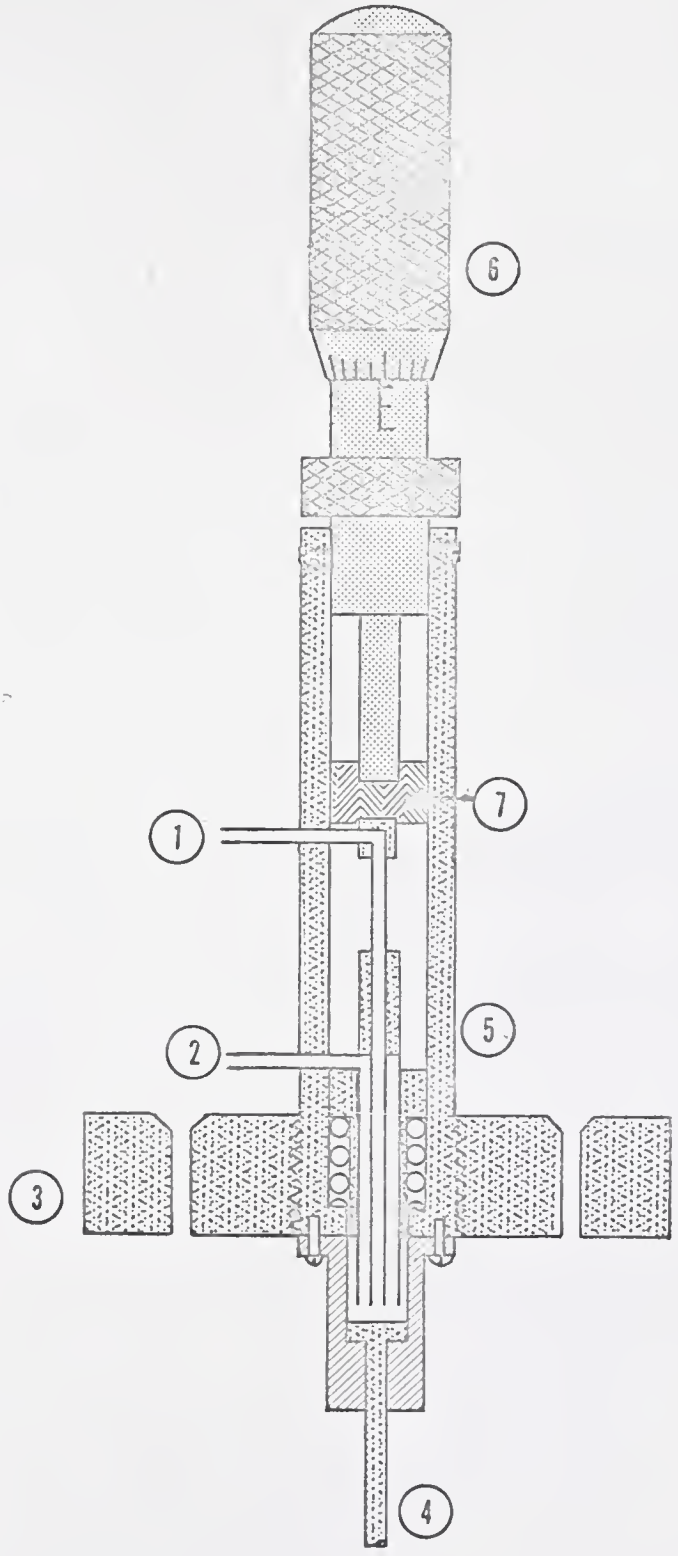
6
7
1
5
2
3
4

plate (3). The actual effective capacitance was determined by the area of the end of the gas inlet tubing, which consisted of an 1/8 in.o.d. brass tube soldered coaxially inside a 1/4 in. brass tube, and the distance from the brass electrode in the recessed LUCITE® insulator at the bottom of the assembly. The concentric tube electrode was spring loaded such that a positive force was always on the rear of the electrode against the micrometer. A TEFLON ® spacer (7) 1/2 in.o.d. by 5/16 in. thick with milled sockets for the anvil of the micrometer and the rear of the concentric electrode was placed between the micrometer and electrode. This maintained alignment of the movable electrode while allowing ease of movement when necessary. The dual-gas inlets (1) and (2) were designed to allow pure helium to flow through the outer cylinder and carrier helium plus sample to flow through the inner cylinder. The purpose was to extend the working range of the detector to very large concentrations. In practice, only the inner cylinder (1) was used for gas flow, while the other gas inlet (2) was sealed off. The sensitivity was reduced considerably when helium flowed through the outer cylinder. Gas entering the cell was vented to the atmosphere through holes in the LUCITE® insulator.

The frequency determining capacitor in the reference oscillator consisted of a 1.3 - 3.1 μμf (160 - 203 E. F. Johnson) butterfly capacitor for fine tuning and 2.7 - 10.8 μμf (160 - 211 E. F. Johnson) butterfly capacitor for coarse tuning. The two capacitors were mounted in parallel on a fiberglass circuit board attached to the chassis on a stand-off arrangement. The advantage of these capacitors over ordinary variable capacitors was that no brush or bearing contacts were present

giving rise to additional impedance in the tank circuit. A phenolic shaft was connected between the rotor shaft and a gear reduction system such that fine tuning of the small capacitor could be easily accomplished. A similar phenolic shaft without gears was attached to the larger capacitor for coarse frequency adjustment. This arrangement was very convenient for adjustment of the reference oscillator frequency to that of the sample oscillator.

The frequency meter and mixer circuit were mounted on the same chassis in a sloping-panel cabinet 10 in.x 18 1/6 in.x 10 13/32 in. The two oscillators were connected to the mixer circuit by means of two short rigid air dielectric coaxial connectors. All three chassis were firmly attached by brackets and screws to a 3/4 in.x 18 in.x 36 in.plywood base. In order to minimize temperature variations, all components were enclosed by construction of a box 12.in x 12.in x 36 in.from 3/8 in. plywood. Hinged doors suitably arranged allowed adjustment of the reference and sample oscillators. The resistors in the frequency meter tended to heat; therefore, ventilation holes were drilled in the front of the sloping-panel cabinet in the vicinity of these resistors, and a 3 1/2 in.hole was cut out of the top of the plywood cabinet. A high velocity fan was mounted above this hole not touching the cabinet. This arrangement worked rather well in cooling the frequency meter circuit. The wooden cabinet was placed on a shock mount (Type 4995-1030 Barrymount, Barry Controls, Watertown, Mass.). This virtually eliminated vibration problems. The power supply connections were made using ordinary hook-up wire.

C. Operating Conditions

The plate voltage supply for the frequency meter and mixer was adjusted to 300 volts. There were several ways to affect the field strength in the detector cell, and this was done by varying the electrode distance in the detector capacitor, the gas pressure in the capacitor, or the power from the oscillator tube. The working conditions were optimized with respect to a 50 µl injection of air into the dilution flask. This corresponded to an initial concentration of 288 parts per million. The best response was obtained with an electrode distance of 0.012 in and an oscillator plate voltage of 390 v. A large increase in field strength resulted in arcing between the electrodes and gave rise to an increase in noise while decreasing the sensitivity drastically. The pressure in the capacitor was assumed to be approximately atmospheric pressure, which was supported by the observation that the response was the same over a wide range of flow rates. The baseline, however, was affected by changes in flow rate, but not the sensitivity.

The frequency chosen for the reference frequency was selected to give greatest linear dynamic range for air and still be within the frequency range of the mixer circuit. The coils (L_R and L_S) in Figure 4 were adjusted by means of a grid-dip meter until both oscillators were operating at about 72 megacycles per second. The exact frequency was not critical as long as both oscillators were oscillating at the same frequency when the r.f. discharge (with only helium carrier) was sustained in the sample cell.

The coils L_2 and L_3 of the diode mixer were extremely critical

and somewhat tedious to wind. It was necessary to wind several coils to obtain a mixer with a wide difference frequency range. The diode mixer and frequency meter circuits gave a linear output with difference frequency from 0.3 to 200 kc.

With helium carrier gas flowing through the detector cell (30 cc - 60 cc per minute), the experimental setup was quite stable. Over a period of several minutes the drift was negligible and the peak-to-peak noise was approximately ± 50 cps.

The carrier gas used was ordinary helium as supplied by Linde Company. A Matheson pressure regulator was used in conjunction with a five-foot piece of 1/8 in.x 0.02 in stainless steel capillary tubing to maintain a well regulated helium flow-rate. In series with this, a metering valve (B-25, Nuclear Products, Cleveland 10, Ohio) and a flow meter (1A-15-1 rotameter, Ace Glass Inc., Vineland, N. J.) were used to control and monitor the final flow rate to the dilution flask and 7.2 (glass ball) - 4.2 (stainless steel ball) (points read at mid-ball position) on the rotameter. This corresponded to a flow rate of 80 cm^3/min as read on a soap-film flow meter.

The filament voltages of the power supplies were turned on to allow the oscillator, mixer, and frequency meter tubes to warm up for about one minute prior to turning the plate voltages on to the values indicated above. The instrumental setup was allowed to warm up for 30 minutes to assure maximum stability. The frequency meter was adjusted to scale No. 6 which corresponded to 4.9 kc full scale, and condenser C_R was adjusted until a difference frequency of zero resulted (if C_R was turned either counter clockwise or clockwise from the position

resulting in a zero difference frequency, the frequency difference increased), and then C_R was turned to give a difference frequency 10 percent of full scale. The sensitivity was then set to the desired value, and C_R was again adjusted to give signal 10 percent of full scale. Then a 50 µl sample of air was introduced through the injection port into the dilution flask by means of a hypodermic syringe, and the emergence of the peak was observed on the frequency meter or recorder. If the signal was first negative and then positive, it was necessary to turn C_R (with helium passing through C_S) until the meter or recorder decreased to zero and then increased again to 10 percent. When the reference oscillator was adjusted to have a higher frequency than the sample oscillator, the samples would normally produce positive peaks with respect to response for air. Once this reference state was established, then the frequency meter was adjusted to the proper scale and working curves were obtained for each sensitivity scale for each gas studied. The detector was checked daily for sensitivity by injecting a reference sample of air, 50 µl by means of a Hamilton 100 µl gas tight syringe fitted with a Chaney adapter adjusted to 50 µl.

D. Potential Detector

The detector based on the change of relative potential difference between two electrodes immersed in the helium r.f. plasma is schematically shown in Figure 9. A Clapp oscillator was used to produce an r.f. discharge within the tank capacitor through which helium carrier gas flows.

A probe inserted in this plasma and the grounded capacitor

Fig. 9 - Schematic Diagram of Oscillator Circuit for Potential Detector.

R_1 = 12k

R_2 = 300 ten turn Helipot

R_3 = 1.2k

R_4 = 12 meg

R_5 = 20 meg

R_6 = 10k

R_7 = 352

B = 225 volts

C_1 = 30 pf (zero temp. coefficient)

C_2, C_3 = 50 pf (zero temp. coefficient)

C_4 = detector cell 4 pf

C_5, C_6 = 2700 pf

L_1 = 22 turns No. 10 silvered wire wound on 3/4 in styrene rod

L_2 = Ohmite Z-28 choke

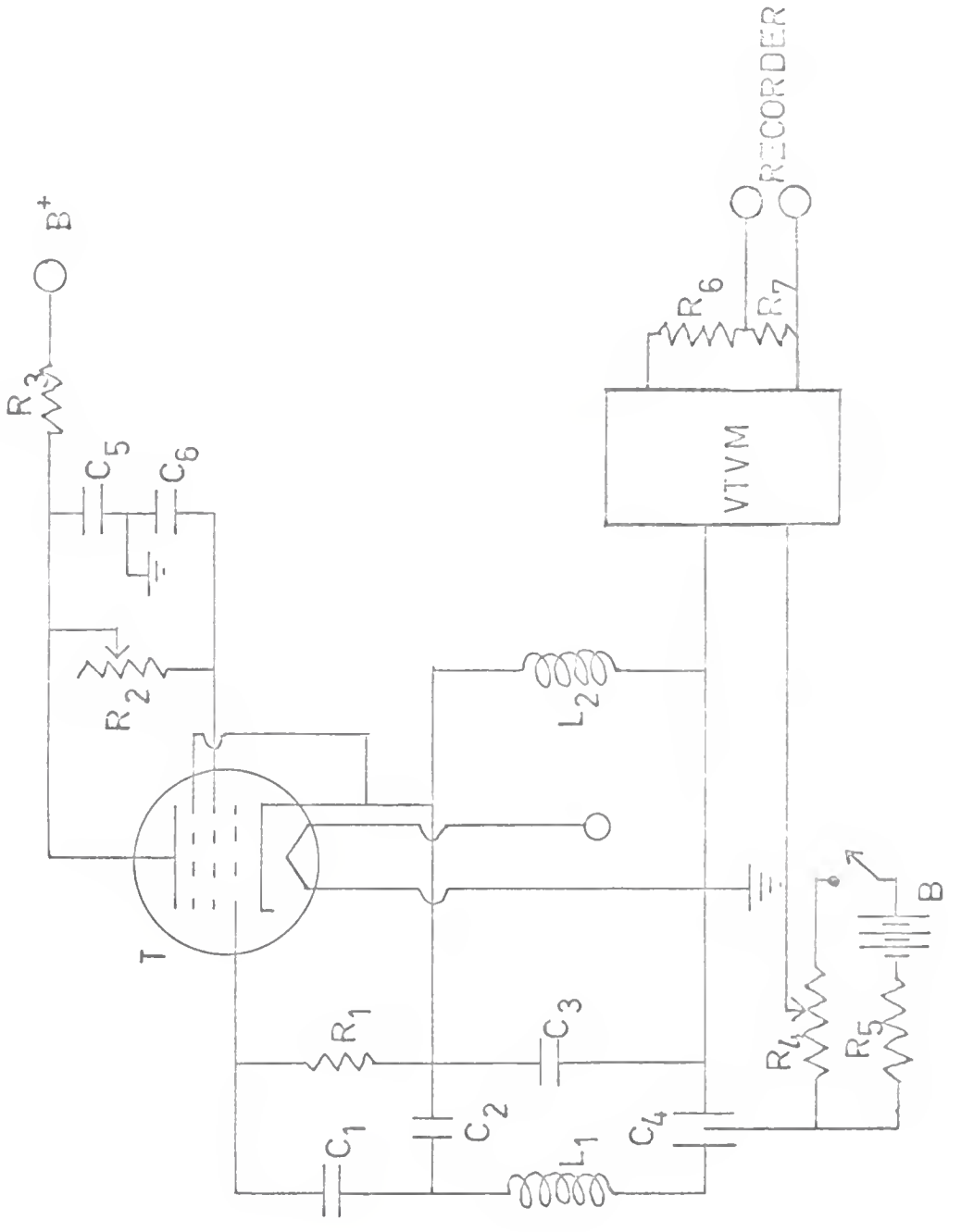
B+
R3
C5
C6
R2
T
R1
C1
C2
C3
L1
L2
C4
R6
R7
RECORDER
VTVM
R4
R5
B

electrode furnished a voltage that could be read on a d.c. vacuum tube voltmeter (Model 220, Keithly Instrument Inc., Cleveland, Ohio). A bucking voltage in series with the probe lead allowed reaction of the baseline voltage. An Ohmite Z-28 r.f. choke was placed in series with the probe and the bucking voltage to attenuate any r.f. oscillations on the d.c. voltage. A voltage dividing network consisting of a 10K ohm fixed resistor and a 3 ohm variable potentiometer were used to reduce the voltage output of the vacuum tube voltmeter and the small voltage (1 mv or less) was measured by a potentiometer recorder. All leads were carefully shielded by use of high quality low capacitance coaxial cable.

Figure 9 shows the schematic circuit of the oscillator. C_4 is the sample cell, and R_2 is a 300K ohm ten-turn Helipot precision resistor which was used to control the power driving the oscillator circuit. This was used to adjust peak voltage obtained from the cell probe.

The cell construction is shown in Figure 10. It consisted of a 1 in. x 1 in. x 1 1/2 in. LUCITE® block in which two 1/8 in. holes were drilled perpendicular to each other and intersecting at the center of the block. The 1/8 in. o.d. stainless steel tube (4) served as an inlet for the carrier gas and sample. The flat electrode and pointed electrode (2) were turned from Monel stock to 1/8 in. x 3/4 in. The point of the tapered electrode was 1/8 in. long with a 35° taper. Copper wire 1/32 in. diameter was silver soldered to the external ends of the monel electrodes to facilitate soldering these to the rest of the circuit using rosin core Pb-Sn solder. A 0.0025 in. hole drilled perpendicular

Fig. 10 - Potential Detector Cell.

1. LUCITE® block 1 in. x 1 in. x 1 1/2 in.
2. Monel electrodes
3. Gold plated No. 22 wire
4. Stainless steel tube 1/8 in. in o.d.

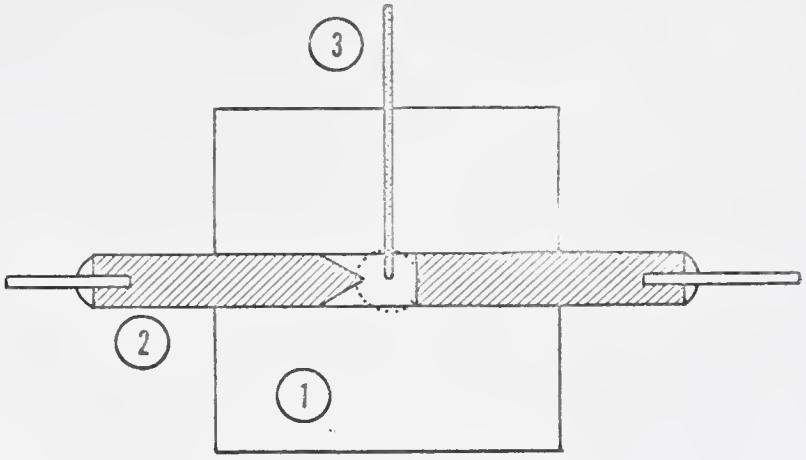
3
2
1

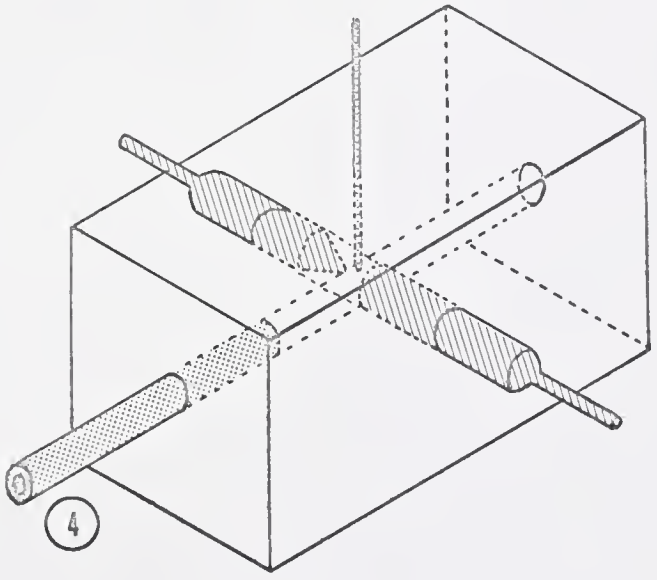
4

to the intersection of gas stream and electrodes allowed the insertion of a No. 22 gold-plated wire between the electrodes. Spacing of the three electrodes was not carefully measured and the design of this cell was certainly not an optimum one, but it demonstrated the feasibility of the method. Roughly the 1/8 in. electrodes were spaced 1/8 in. apart while the wire probe (3) was positioned parallel to the face of the flat electrode. The distance between the flat electrode and the wire probe was about 1/32 in. to 1/16 in. with the tip of the wire slightly above the center of the gap between the electrodes as shown in Figure 10.

E. Operating Conditions

The operating conditions for this arrangement were obtained by maximizing response for a 10 µl injection of air into the dilution flask. This corresponded to an initial concentration of 45.7 parts per million of air in helium carrier. The optimum conditions for the cell described was a flow rate of 5.2 (stainless steel ball) - 9 (glass ball) of a flowmeter (size 1A15-1, Ace Glass Inc.). The B+ voltage was adjusted to 390 volts or 335 volts and 890 or 840 on the ten turn resistor dial. The grid resistor, R_2, had values ranging from 33K to 34.8K ohms. These resistance values were arrived at by decreasing the grid resistor values until a stable voltage was indicated on the VTVM. This meant an r.f. discharge was then established in the cell. The r.f. discharge increased in size when R_2 was decreased. The resistance, R_2, was decreased until a maximum voltage of 40 to 60 volts was indicated. The resistance was further decreased until the voltage again dropped to roughly 50 percent of the peak voltage or to 20 to 30 volts. This meant that both the probe

and the ground reference electrode were then immersed in the r.f. glow discharge.

When a sample of air was introduced in the carrier gas, an increase in voltage was observed. If a very large sample was introduced, the voltage first increased then decreased to the point where the discharge was sometimes extinguished depending on the size of sample injected. Working curves were measured over a range of voltages varying from reference voltage to maximum voltage.

A 225 volt dry cell battery, a 12 megohm variable potentiometer, and a 20 megohm fixed resistor made up the bucking voltage network. This was enclosed, together with the previously mentioned r.f. choke, in a 7 in.x 6 in.x 6 in.aluminum box for shielding. An on-off switch for the battery and TEFLON® insulated feed through connectors completed the suppression network.

The frequency of the oscillator was 25 Mcs. This choice was not completely arbitrary because the oscillator frequency determined the visual size of the glow discharge for the cell arrangement and other working conditions.

IV. RESULTS AND DISCUSSION

A. Frequency Detector

The response of the frequency detector was determined for the following gases: Air, N_2, Ar, CO, H_2, CO_2, O_2, NH_3, NO_2, SO_2, CH_4, CH_3Cl, C_2H_6, n-C_3H_8, n-C_4H_{10}. In Table 1 the limit of detection and useful dynamic range of 15 gases in helium carrier gas are given.

The analytical curves are plotted on log-log coordinates in order to compress the curves to a convenient size. Any deviation from unity slope indicates non-linearity in response. Figures 11 through 18 are the analytical curves obtained.

It seems evident that the gases with a negative (-) response either decrease the number of electrons by a dilutional process and/or electron capture mechanism. Ionization should lead to an increase in the number of electrons in the plasma. Competition of all these mechanisms, i.e.

$$He^* + S \rightarrow S^+ + e^- + He$$

$$S^+ + e^- \rightarrow S$$

$$S + e^- \rightarrow S^-$$

$$S \rightarrow \text{dilution of carrier}$$

is possible.

It should be noted that a 50 microliter sample of air was injected daily to see if the response was reproducible. For a series of ten injections of 50 μl of air (injections were made over a 10-minute period),

the relative standard deviation was 3.4 percent. For a large number of injections of 50 µl of air over a period of two months, the relative standard deviation was slightly less than 9 percent.

Table 1

Limits of Detection and Useful Dynamic Range for Several Gases Using the Frequency Detector

Gas	Limit of Detection ppm	Useful Dynamic Range	Response[a]
NO_2	0.04	10^3	-
SO_2	0.6	10^4	-
CO	6.0	10^3	-
N_2	6.0	10^3	-
CO_2	3.0	10^4	-
NH_3	60.0	5×10^2	-
H_2	60.0	5×10^2	-
Air	4.0	5×10^3	-
O_2	2.0	10^4	-
CH_3Cl	2.0	10^4	-
CH_4	2.5	10^3	-
C_2H_6	0.9	10^3	+
$n\text{-}C_3H_8$	1.0	10^3	+
$n\text{-}C_5H_{10}$	1.0	10^2	+
Ar	100.0	5×10^2	+

[a](+) means frequency increases due to sample gas in helium carrier gas. Air was used as the reference gas for all measurements.

Fig. 11 - Analytical Curve for NO_2.

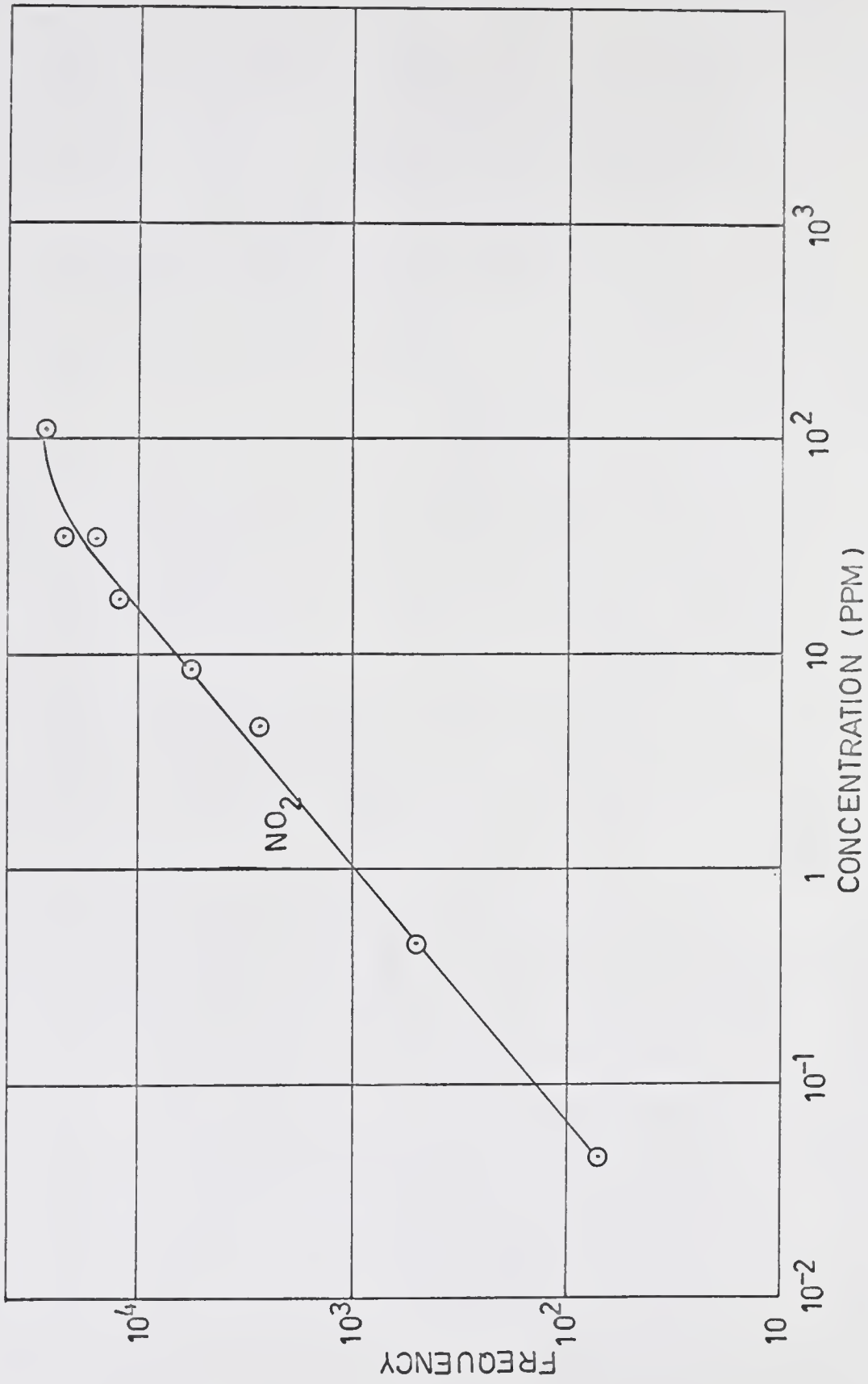
FREQUENCY
10^4
10^3
10^2
10
NO_2
10^{-2}
10^{-1}
1
10
10^2
10^3
CONCENTRATION (PPM)

Fig. 12 - Analytical Curve for CH_3Cl.

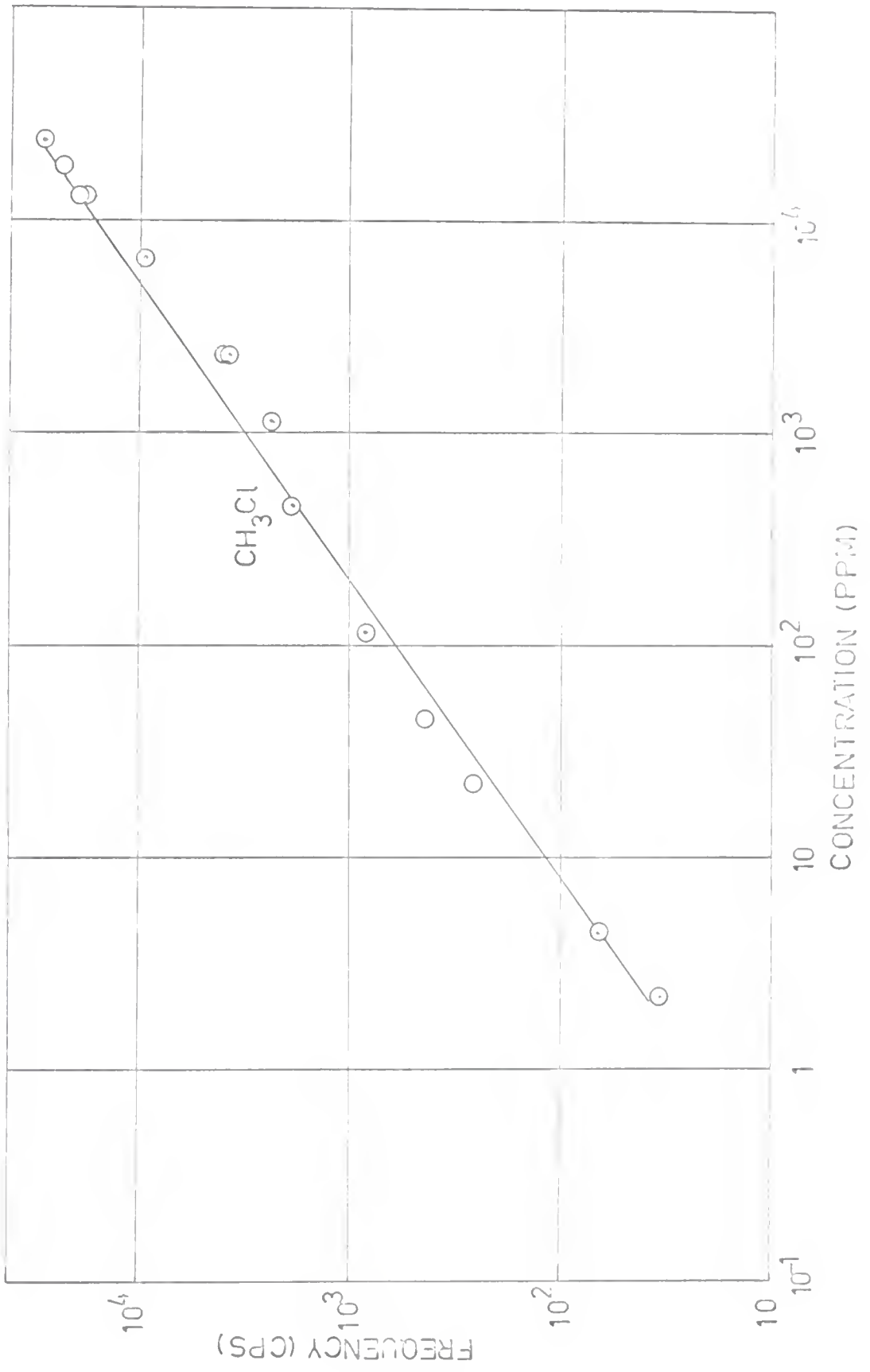
FREQUENCY (CPS)
10^4
10^3
10^2
10
10^{-1}
1
10
10^2
10^3
10^4
CONCENTRATION (PPM)
CH_3Cl

Fig. 13 - Analytical Curves for $n\text{-}C_3H_8$ and O_2.

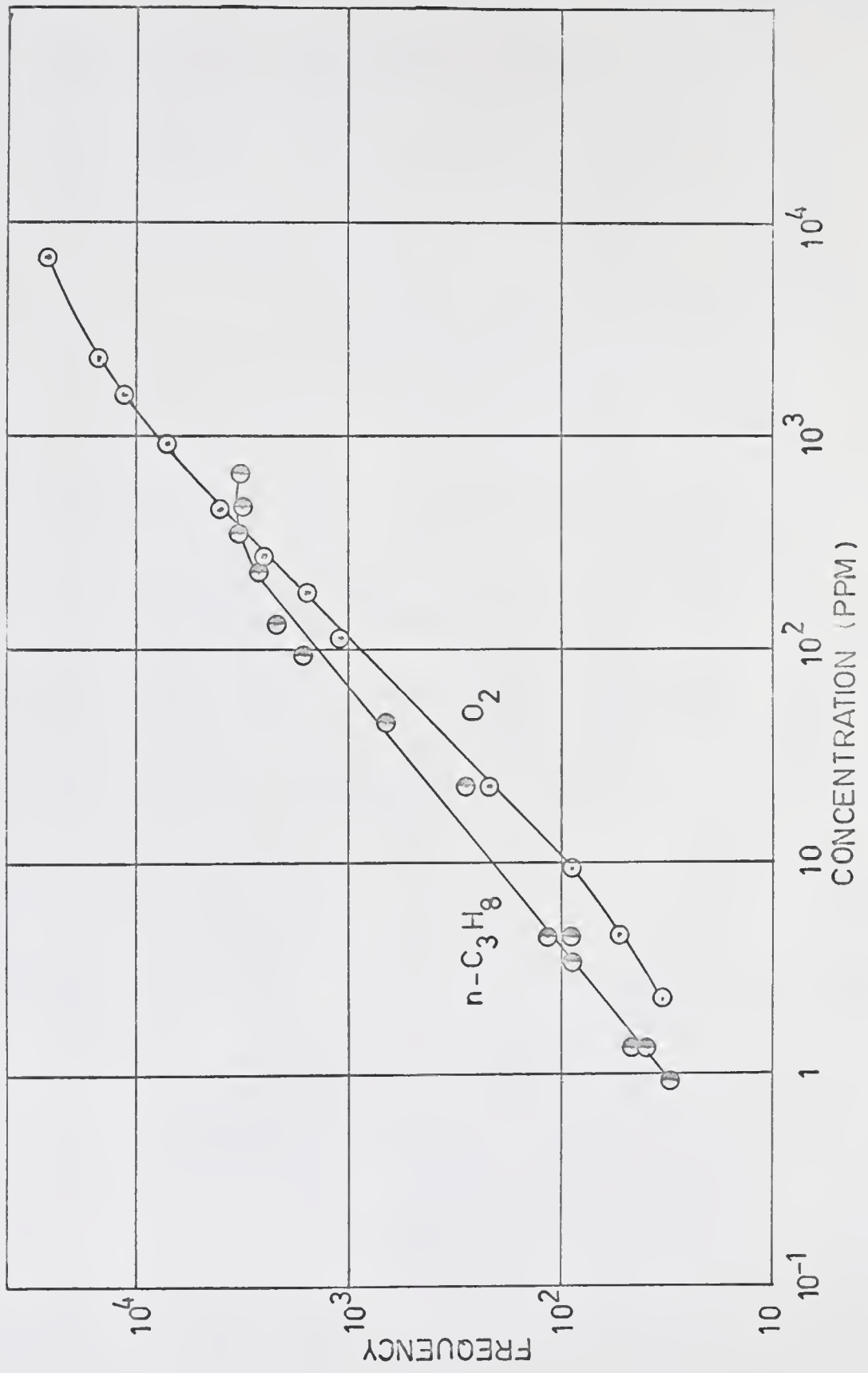
FREQUENCY
10^4
10^3
10^2
10
10^{-1}
1
10
10^2
10^3
10^4
CONCENTRATION (PPM)
O_2
$n-C_3H_8$

Fig. 14 - Analytical Curves for CO and H_2.

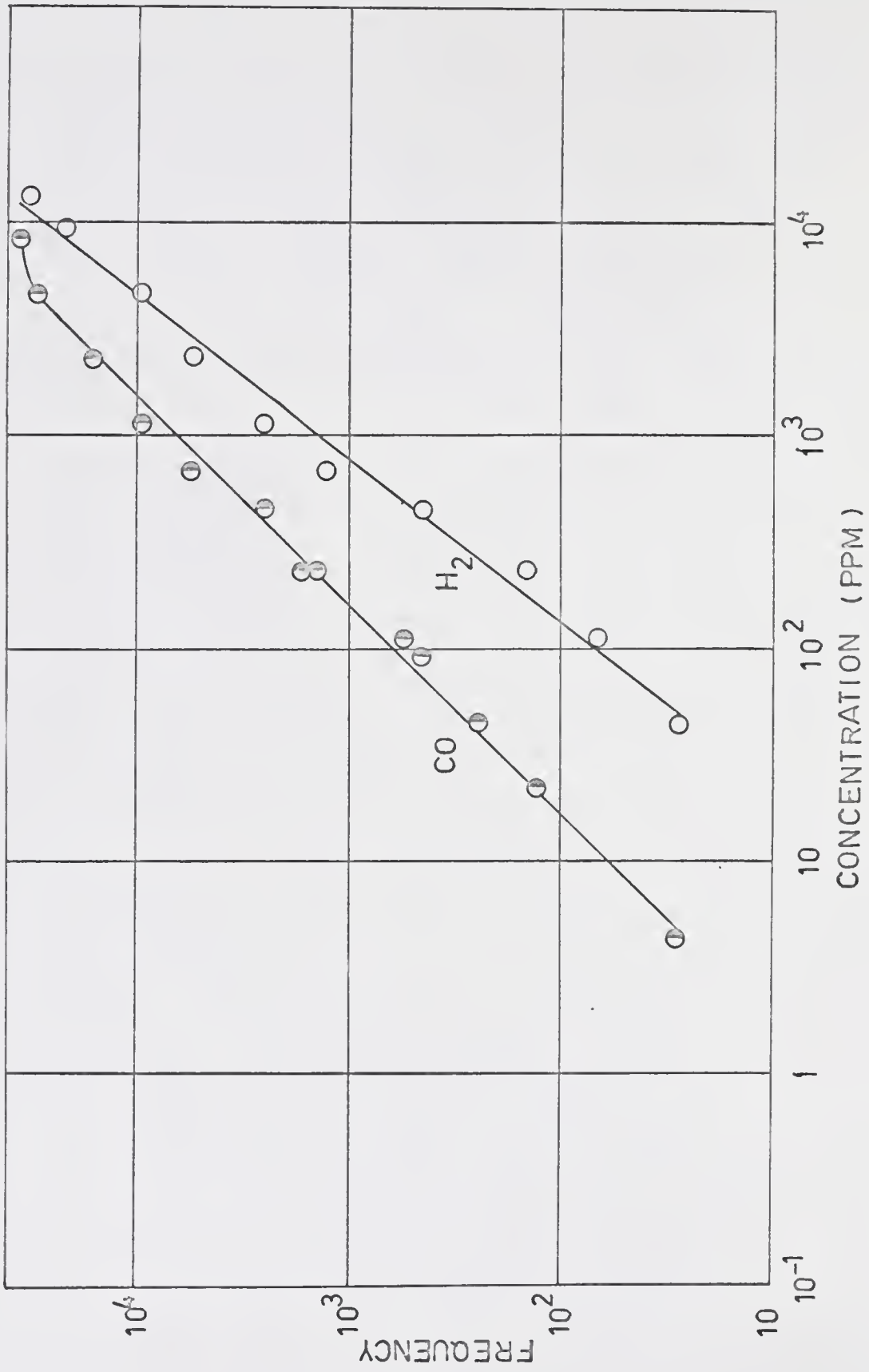
FREQUENCY
10^4
10^3
10^2
10
10^{-1}
1
10
10^2
10^3
10^4
CONCENTRATION (PPM)
H_2
CO

Fig. 15 - Analytical Curves for CO_2 and NH_3.

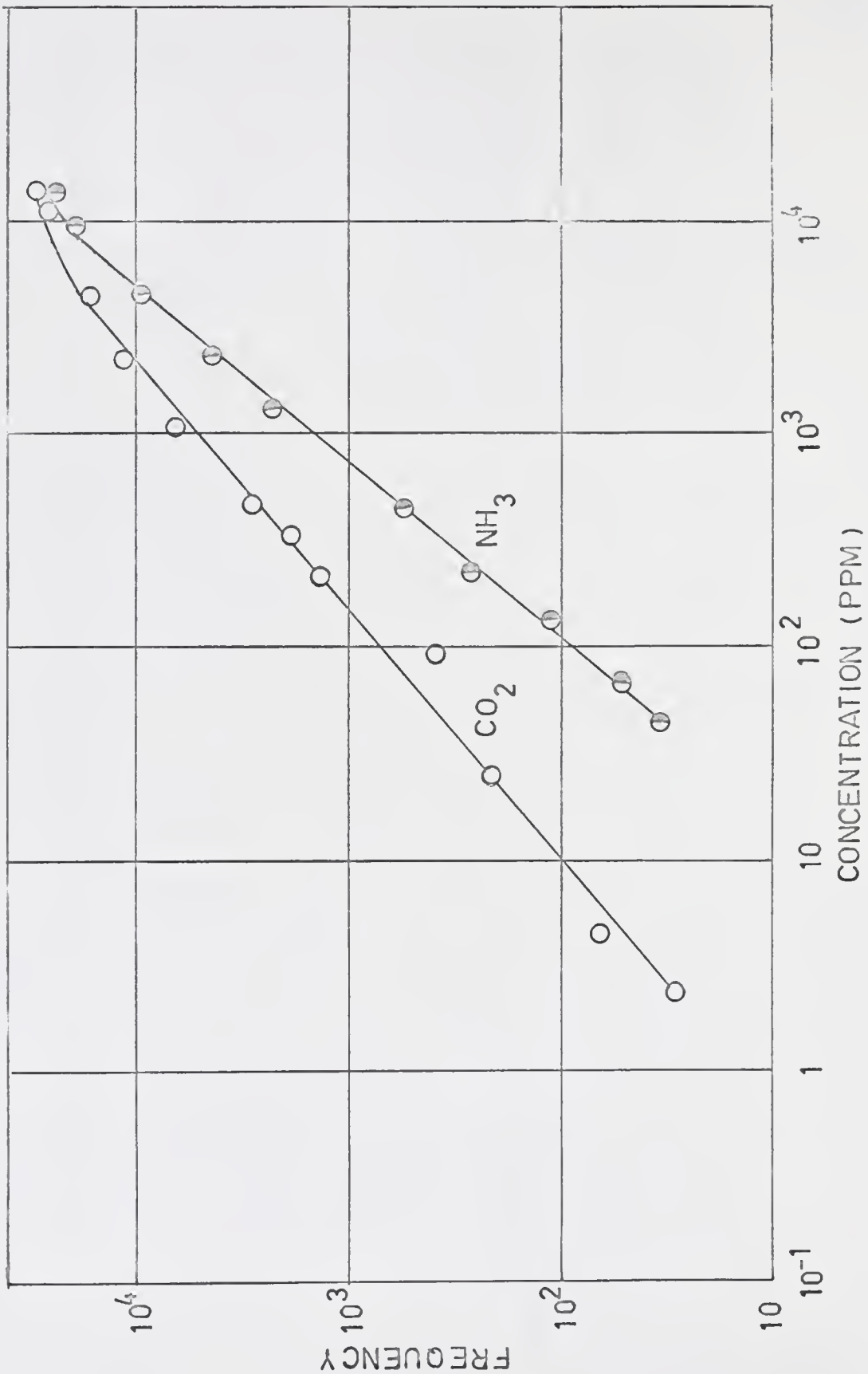
FREQUENCY
10^4
10^3
10^2
10
10^{-1}
1
10
10^2
10^3
10^4
CONCENTRATION (PPM)
NH_3
CO_2

Fig. 16 - Analytical Curves for N_2, CH_4 and Ar.

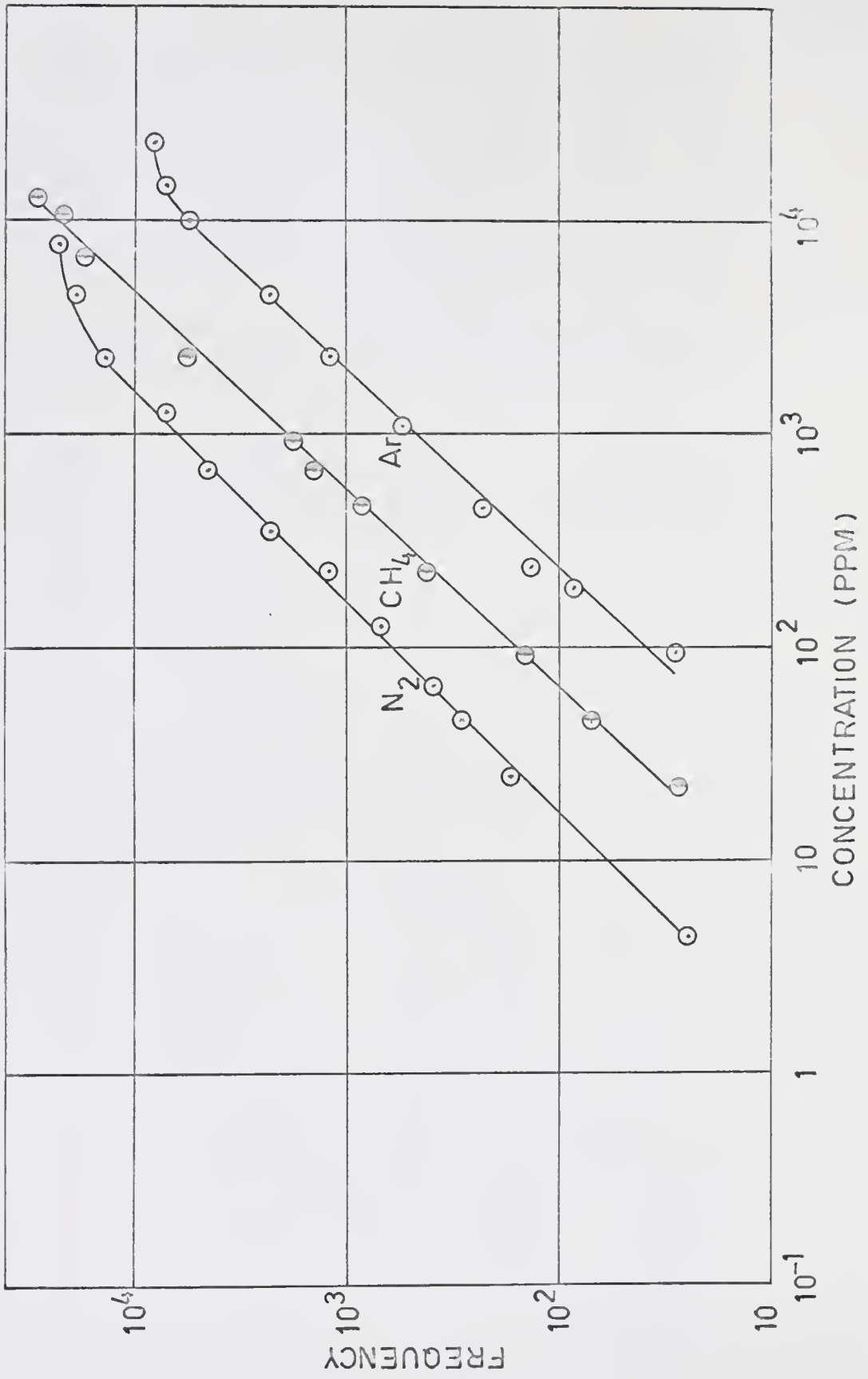
FREQUENCY
10^4
10^3
10^2
10
10^{-1}
1
10
10^2
10^3
10^4
CONCENTRATION (PPM)
Ar
CH_4
N_2

Fig. 17 - Analytical Curves for SO_2 and C_2H_6.

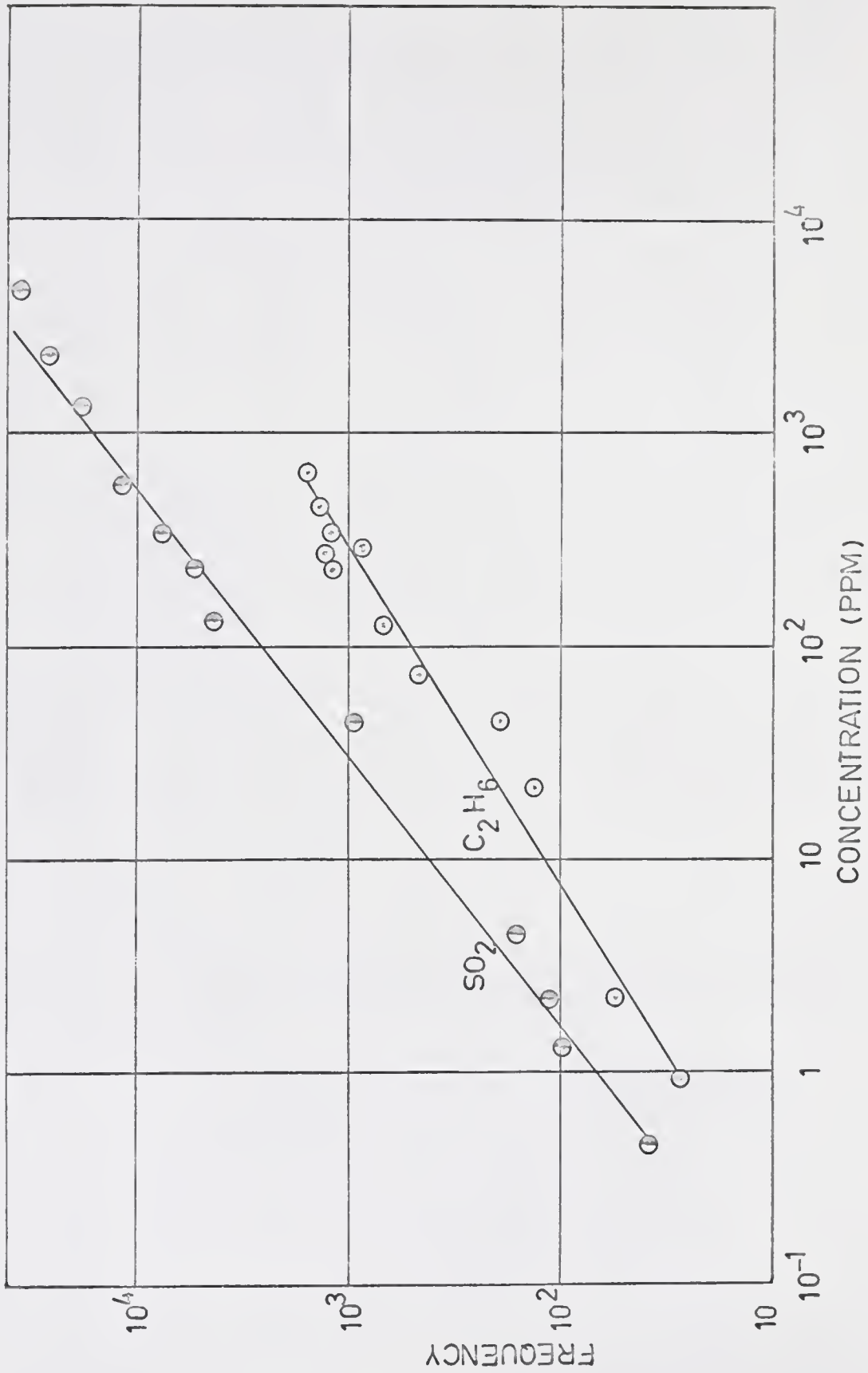
FREQUENCY
10^4
10^3
10^2
10
10^{-1}
1
10
10^2
10^3
10^4
CONCENTRATION (PPM)
C_2H_6
SO_2

Fig. 18 - Analytical Curves for $n\text{-}C_4H_{10}$ and Air.

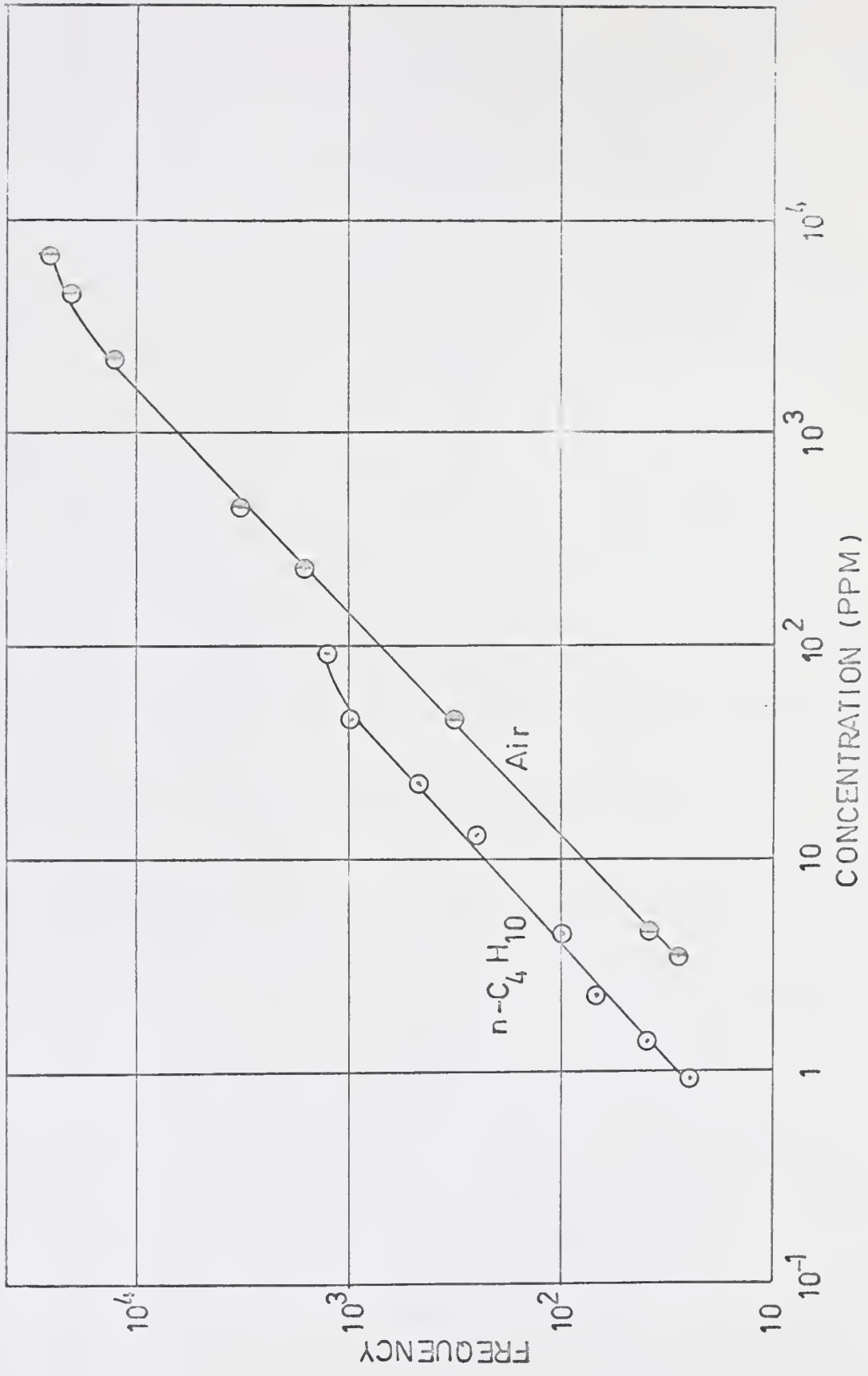
FREQUENCY
10^4
10^3
10^2
10
10^{-1}
1
10
10^2
10^3
10^4
CONCENTRATION (PPM)
Air
$n\text{-}C_4H_{10}$

B. Potential Detector

Working curves for the potential detector were determined for the following gases: SO_2, N_2O, CO_2, Ar, CO, Air, N_2, and H_2. The limit of detection and useful dynamic concentration range for light gases or helium are given in Table 2. The analytical curves were plotted on log-log coordinate paper in order to compress the curves. Any deviation from unity slope indicates non-linearity in response. Figures 19 through 21 are the working curves obtained for this detector. All gases responded by increasing the voltage output. Again, air was chosen as a reference gas.

This detector was not as reproducible as the frequency detector. The baseline voltage drifted slowly over a several-day period. This was attributed to electrode reactions at the gold-plated probe which showed evidence of a deposition of some type on the probe. It is believed that the electrodes should be "aged" longer to achieve a more drift-free state. Drift was negligible over a one-day period, and each determination was made within a half day so that baseline drift was negligible for each sample.

Table 2

Limits of Detection and Useful Dynamic Range for Several Gases Using the Potentiometric Detector

Gas	Limit of Detection (ppm)	Useful Dynamic Range
N_2O	0.1	10^4
SO_2	0.07	10^4
CO_2	0.8	10^4
Air	1.0	5×10^3
CO	6.0	10^3
N_2	7.0	5×10^2
Ar	80.0	5×10^2
H_2	70.0	10^2

Fig. 19 - Analytical Curves for Air, CO, and H_2.

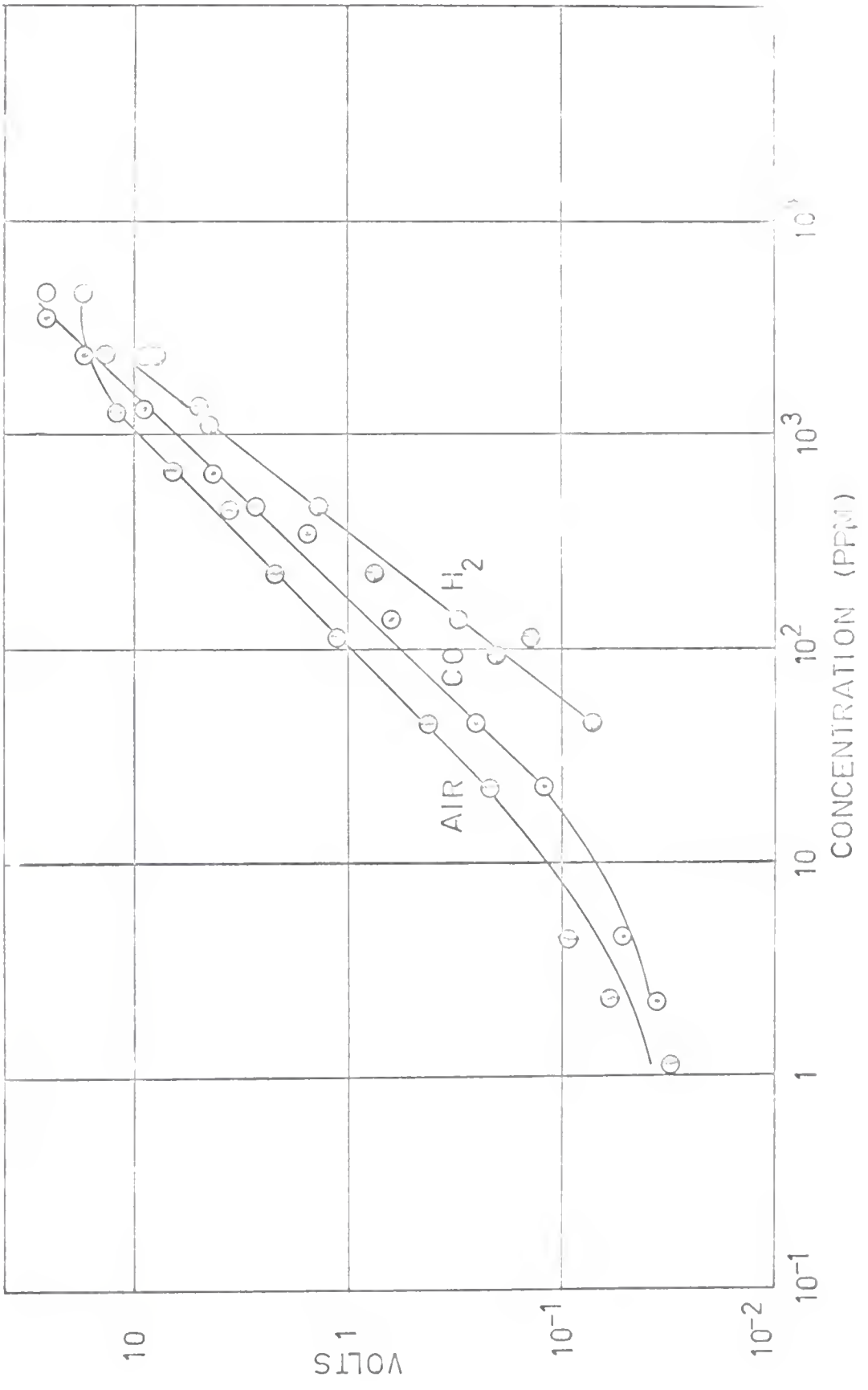
VOLTS
10
1
10^{-1}
10^{-2}
10^{-1}
1
10
10^{2}
10^{3}
CONCENTRATION (PPM)
AIR
CO
H_2

Fig. 20 - Analytical Curves for SO_2 and N_2.

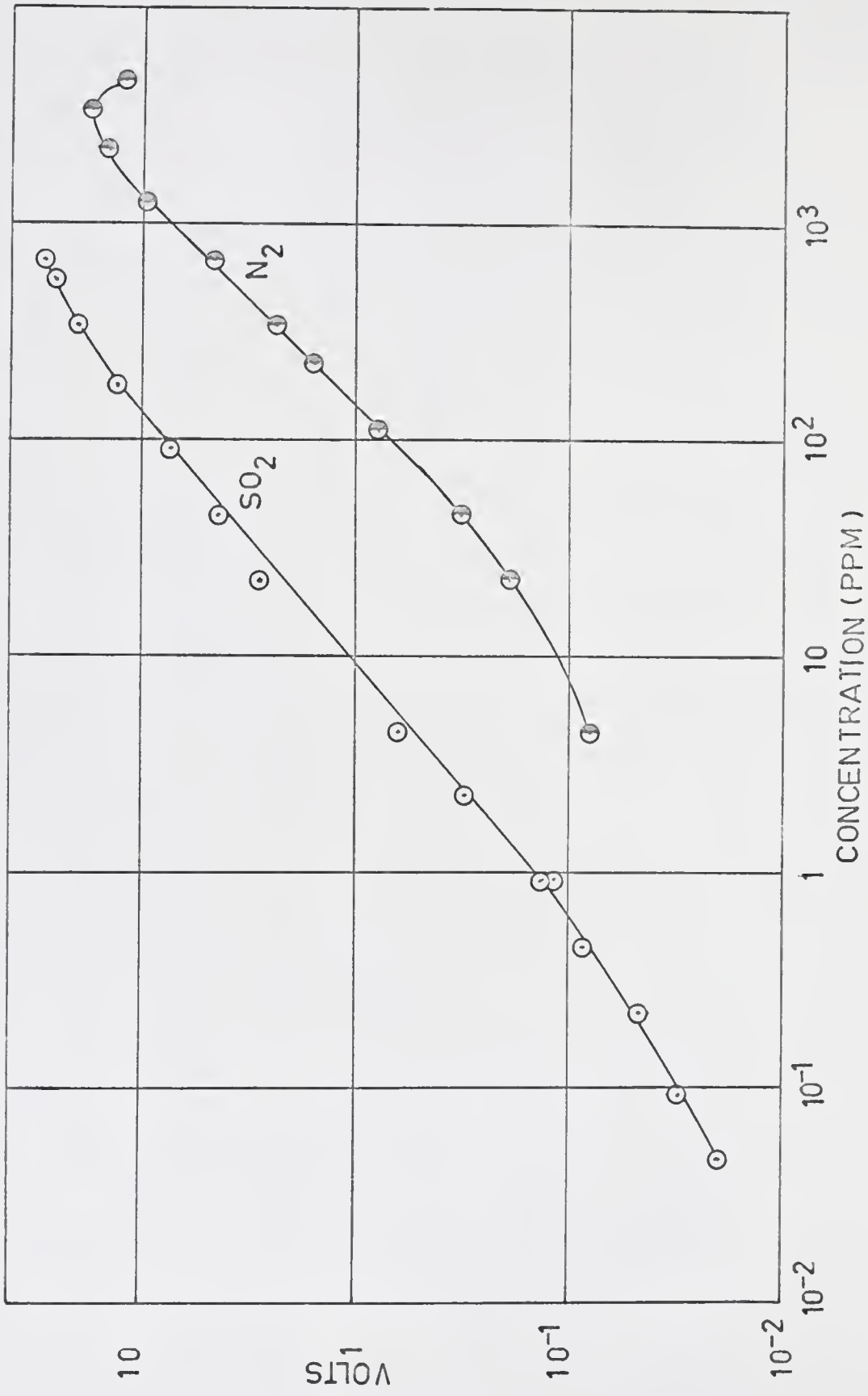
VOLTS
10
10^{-1}
10^{-2}
10^{-2}
10^{-1}
1
10
10^{2}
10^{3}
CONCENTRATION (PPM)
N_2
SO_2

Fig. 21 - Analytical Curves for N_2O, CO_2, and Ar.

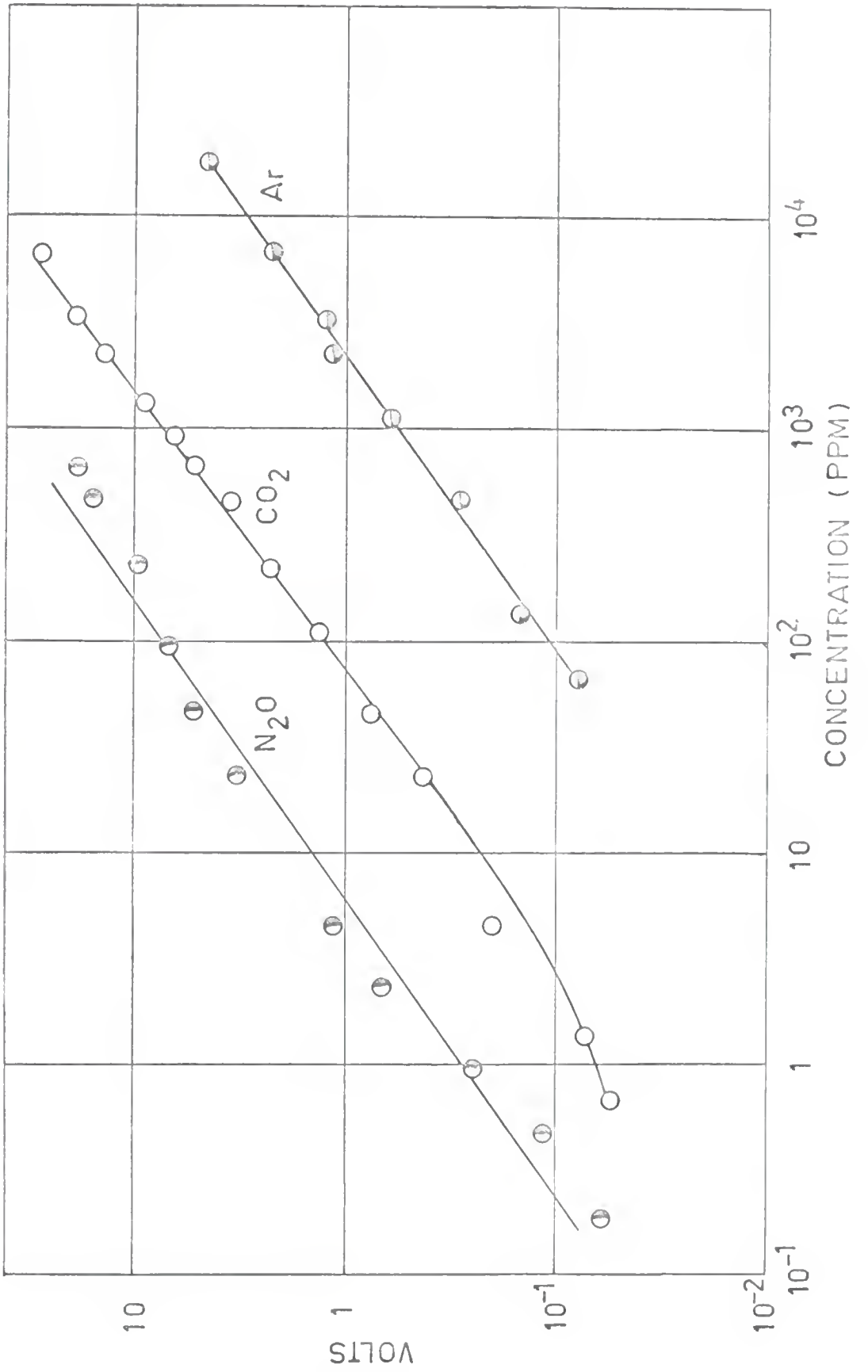
Ar
CO_2
N_2O
VOLTS
10
1
10^{-1}
10^{-2}
10^{-1}
1
10
10^2
10^3
10^4
CONCENTRATION (PPM)

C. Comparison of the Two r.f. Detectors

It is difficult to compare the two detectors because the potential detector was not completely optimized. However, some comparisons can still be made. In Table 3, the frequency detector is compared with the potential detector. Within an order of magnitude the performance of the two detectors is about the same for the gases listed.

In Table 4, the two detectors are compared with other detectors commonly used in gas chromatography. The data in Table 4 indicate that the two detectors are as sensitive as the most sensitive ionization detectors available. They are inexpensive to construct and have wide useful dynamic ranges (10).

D. Further Work Needed on r.f. Detectors

If the Clapp oscillators were reconstructed using solid state components, then noise level and drift should decrease greatly. Greater overall stability would probably result by using a commercial mixer and a commercial frequency meter.

A new cell design for the potential detector would be advantageous. The cell depicted in Figure 10 is far from an optimum design. In principle, this detector is nearly the same as that reported by Karmen and Bowman (5) (6). A concentric cell as described by them could be used if the vacuum tube voltmeter is arranged to measure the potential difference across the whole series coil-capacitance network. An alternative cell could be constructed according to Figure 22. This cell should have an even smaller volume than the cell described by Karmen and Bowman (5) (6). Ideally, Invar or Elinvar should be used to make the

Table 3

Comparison of Frequency and Potential Detectors

Gas	Limit of Detection		Useful Dynamic Range	
	Frequency ppm	Potential ppm	Frequency	Potential
SO_2	0.6	0.07	10^4	10^4
CO	6.0	6.0	10^3	10^3
N_2	6.0	7.0	10^3	5×10^2
CO_2	3.0	0.8	10^4	10^4
H_2	60.0	70.0	5×10^2	10^2
Air	4.0	1.0	5×10^3	5×10^3
Ar	100.0	80.0	5×10^2	5×10^2

Table 4

Comparison of Frequency and Potential Detectors With Other Detectors

Detector Type	Minimum Detectable Conc.	Carrier Gas	Construction	Anal. Curve	Substance Detectable
Katharometer	$10^{-4}(H_2)$	N_2	Simple	Linear	Org. & Inorg.
Flame Ionization	10^{-11}(propane)	H_2	Complicated	Linear	Organic
Argon	10^{-12}(propane)	Ar	Complicated	Linear to certain concen.	Org. & Inorg.
Cross Section Ionization	10^{-4}(propane)	H_2	Complicated	Linear	Org. & Inorg.
Electron Capture	$10^{-13}(CCl_4)$	Ar	Complicated	Linear	Halogen & Oxygen Comps.
Frequency Detector	$10^{-13}(NO_2)$	He	Complicated	Linear	All Permanent Gases
Potential Detector	$10^{-12}(SO_2)$	He	Simple	Linear	All Permanent Gases

tank circuit components in order to reduce thermal drift. It is imperative that the cell should be unsymmetrical.

The r.f. discharge is (according to Karmen and Bowman)(6) 90 percent destructive to organic samples passing through the discharge. Use may be made of this property by using the discharge as a pyrolysis cell. By injecting the sample into the discharge cell, fragmentation should occur and then passing the effluent gases through a packed column and then through a detector, the sample should give a "fingerprint" of the organic material sampled.

If a flame is placed within the capacitor cell using a potential readout as in the potential detector, this could result in a sensitive gas chromatographic detector and a means of studying flame processes. Such a detector has already been demonstrated to have considerable analytical use.

Fig. 22 - Proposed Cell for the Potential Detector.

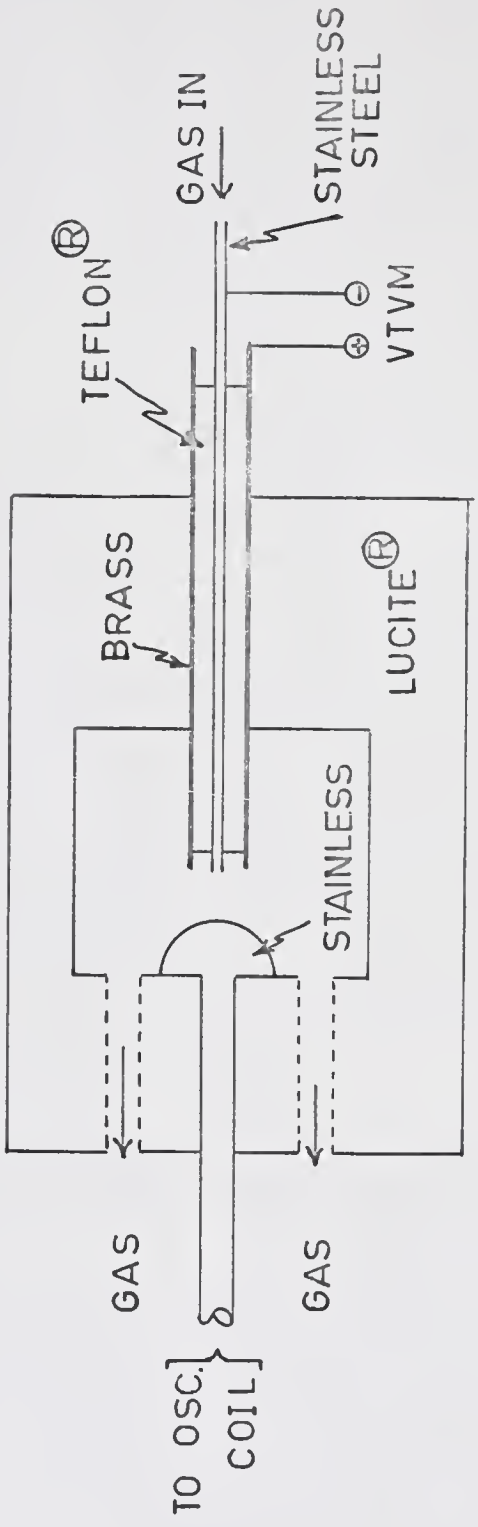
GAS IN
STAINLESS STEEL
TEFLON®
VTVM
BRASS
LUCITE®
STAINLESS
GAS
GAS
TO OSC. COIL

BIBLIOGRAPHY

1. Turner, D. W. NATURE, 181, 1265 (1958).

2. Winefordner, J. D., Steinbrecher, D., and Lear, W. E. Anal. Chem., 33, 515 (1961).

3. Von Hippel, A. R. Dielectrics and Waves, John Wiley & Sons, New York (1954), p. 262.

4. Francis, G. Ionization Phenomena in Gases, Butterworths Scientific Publications, London (1960), p. 136.

5. Karmen, A., and Bowman, R. L. Anals. New York Academy of Sciences, 72, 714 (1959).

6. Karmen, A., and Bowman, R. L. Gas Chromatography, Sec. Int. Symp. Anal. Instr. Div. Instr. Soc. of America, June 1959, Academic Press, New York (1961), p. 65.

7. Hampton, W. C. Journal of Gas Chromatography, 3, 217 (1965).

8. Winefordner, J. D., Williams, H. P., and Miller, Anal. Chem. 37, 161 (1965).

9. Lovelock, J. E. Anal. Chem., 33, 162 (1961).

10. Seiyama, T., and Kagawa, S. Anal. Chem., 38, 1069 (July, 1966).

BIOGRAPHICAL SKETCH

Howard Person Williams was born in Wilson County, North Carolina, and attended public school in Wilson. In September of 1950, he entered East Carolina College. He joined the United States Air Force in May, 1953. On January 14, 1956, the author married Joan Calvert. Upon separation from the service in May, 1957, he reenrolled at East Carolina College and received a Bachelor of Arts degree in May, 1960, after completing the requirements for a major in Chemistry and in Mathematics.

After entering the Graduate School of the University of Florida in June, 1960, the author held the position of graduate assistant. In April, 1963, he received a Master of Science degree with a major in Chemistry. On January 4, 1964, he reentered the Graduate School of the University of Florida in order to work toward a Doctor of Philosophy degree.

Mr. and Mrs. Williams have two sons, Howard Person Williams, Jr., and Michael Calvert Williams.

This dissertation was prepared under the direction of the chairman of the candidate's supervisory committee and has been approved by all members of that committee. It was submitted to the Dean of the College of Arts and Sciences and to the Graduate Council, and was approved as partial fulfillment of the requirements for the degree of Doctor of Philosophy.

December 17, 1966

E. Ruffin Jones

Dean, College of Arts and Sciences

Dean, Graduate School

Supervisory Committee:

J. E. Wenzel

Chairman

P. J. Hanrahan

[illegible] for F N Rhines

[illegible]

[illegible] for G. M. Schmid

HHI7-A